



Electrode material based on reduced graphene oxide (rGO)/transition metal oxide composites for supercapacitor applications: a review

R. Kumar¹ · R. Thangappan¹

Received: 27 October 2021 / Accepted: 9 December 2021 / Published online: 4 January 2022
© Qatar University and Springer Nature Switzerland AG 2021

Abstract

The supercapacitor is a modern electrochemical energy storage technology, exhibiting high specific capacitance, long-term cycle stability, rapid charge rates, high power density, and low cost. Nanostructured materials such as nanocarbons, metal oxides, graphene nanosheets, and conducting polymers are used for energy storage applications in recent years. The most fascinating features of 2D reduced graphene oxide-based electrode materials, such as high surface area, superior electrical conductivity, good chemical stability, and excellent mechanical behavior, make them suitable material for supercapacitor devices. Also it attributes the enhancement in specific capacitance, excellent cyclic stability, and high energy density of the composite electrodes that are mainly due to the interconnected conductive network of the composite as well as the synergistic effect of the metal oxide and graphene. This review contains the most significant developments in rGO-TMO-based materials for supercapacitor electrodes, depending on the number of metal oxide composites paired with rGO, i.e., metal oxide, binary metal oxide, and ternary metal oxides. The method of synthesis and supercapacitor performances of rGO and transition metal oxide composites are reviewed. Additionally, a comparison of the rGO composite's synergistic effects on supercapacitor performance in terms of specific capacitance, energy density, power density, rate capability, and cycle stability are tabulated.

Keywords Reduced graphene oxide (rGO) · Supercapacitors · Transition metal oxide · Specific capacitance · Composite

1 Introduction

The demand for energy storage will be on the rise as the progress of electronic technology has grown in the past years. Only a few energy storage solutions stand out from the rest of the field. Electrochemical capacitors (ECs) have now become a substantial area of study due to their desirable characteristics, such as fast charge and discharge rates, energy density, power density, and long cycle life [1–3]. Supercapacitors are also referred to as electrochemical capacitors. According to this classification, super capacitors are categorized as electrical double-layer capacitors (EDLCs) and pseudo-capacitors, depending on their charging storage method [4]. Carbon-based materials, such as carbon nanotubes [5, 6], activated carbon [7], carbon fibers [8], and graphene [9], are widely used as EDLC

materials, resulting in high conductivity and specific surface area [10]. Metal oxides, such as MnO₂ [11], Co₃O₄ [12], NiO [13], Fe₂O₃ [14], MoO₂ [15], RuO₂ [16], V₂O₅ [17], SnO₂ [18], TiO₂ [19], polymers [20], and other materials [21] have been used to enhance the specific capacitance of pseudo-capacitors.

Most carbon compounds, such as graphene oxide (GO) and reduced graphene oxide (rGO), are made from naturally occurring carbon precursors, such as pyrolyzed graphite and pyrolyzed coal. Graphene is well-known for its electrical conductivity, while graphene oxide (GO) is more likely to behave as an insulator in electrical applications. A number of different techniques for synthesizing graphene derivatives have been developed, but low-cost; high-yield manufacturing continues to be a significant challenge. To make graphene derivatives for high-end applications on a large scale, precursor minerals such as graphite, coal, coke, anthracite, and biomass are necessary [22]. Graphene is a carbon allotrope that has the form of a 2D dimensional hexagonal lattice on an atomic scale, and has a specific surface area of 2630 m²/g. It is the most abundant carbon allotrope on the planet. Graphene is

✉ R. Thangappan
thangappan@periyaruniversity.ac.in

¹ Advanced Functional Materials for Energy Lab, Department of Energy Science & Technology, Periyar University, Salem, Tamil Nadu, India

dissimilar to activated carbon and carbon nanotubes. The varied accessible surface area of graphene in EDLCs is due to its monolayer 2D lattice structure of carbon atoms. Because of its high conductivity and mechanical stability, graphene is a suitable substrate for active materials such as faradaic materials with pseudo-capacity [23].

In terms of cycle stability, graphene oxide performed much better than graphene. Graphene oxide has superior performance and a lower cost when compared to graphene as an electrode material in supercapacitors [24]. Since the early nineteenth century, the techniques of Brodie, Staudenmaier, Offeman, and modified Hummers for generating graphene oxide (GO) have been exploited. These chemical processes, on the other hand, require the use of a large number of concentrated acids and powerful oxidants, which may result in a number of potential safety risks [25]. Nowadays, the modified Hummer's technique is the most frequently used method for synthesizing GO. The most typical technique is to treat graphite powder with a solution of sodium nitrate, potassium permanganate, and sulfuric acid. While GO readily dissolves in water, it also dissolves in organic solvents [26].

GO includes oxygen functionalities (epoxy, hydroxyl, carboxyl, and carbonyl groups) on its surfaces and edges, which aid in the attachment of metallic nanoparticles for use in energy-related applications by forming hydrogen bonds with them. The reduction product of graphene oxide (GO) is known as reduced graphene oxide (rGO). It reduces GO using the following methods: chemical reduction, thermal annealing/reduction, microwave reduction, and laser reduction. These are widely applied to eliminate functional groups containing oxygen from GO surfaces [27–33]. New advancements in two-dimensional graphene-based materials are being made in the electrode materials for supercapacitors. In order to improve the active sites of electrode materials that have been blended with various metal oxides, metal hydroxides, metal sulfides, mixed metal oxides, and ternary metal composites [33, 34]. Metal oxide materials exhibit pseudo-capacitance behavior because it leads to very poor stability and conductivity performance of the device [14, 15]. To overcome the performance many researchers are investigated in 2D materials which can improve the conductivity of metal oxides and bounds the agglomeration and also restacking of two dimensional materials. The hybridization of metal oxide with carbonaceous materials, particularly reduced graphene oxide, has a synergistic effect that increases electrical conductivity and improves the kinetics of ions and electron transport at the electrode/electrolyte interface as well as the interior of the electrodes. Because rGO acts as a current collector and can also absorb a large amount of charge generated by electrostatic interactions, therefore rGO-based composites improve the overall electrochemical performance. And also many authors precisely researched about rGO-based binary, ternary composites in

order to improve the specific capacitance, energy density, and power density of the devices [25, 26].

This review discusses current and future energy storage technologies problems and possibilities. The progress made in the area of energy storage devices such as pseudo-supercapacitors, asymmetric supercapacitors, and hybrid supercapacitors, using reduced graphene oxide/transition metal oxide composite mechanism of action, and enhanced energy storage capacity are the main focus.

2 Modified Hummers method

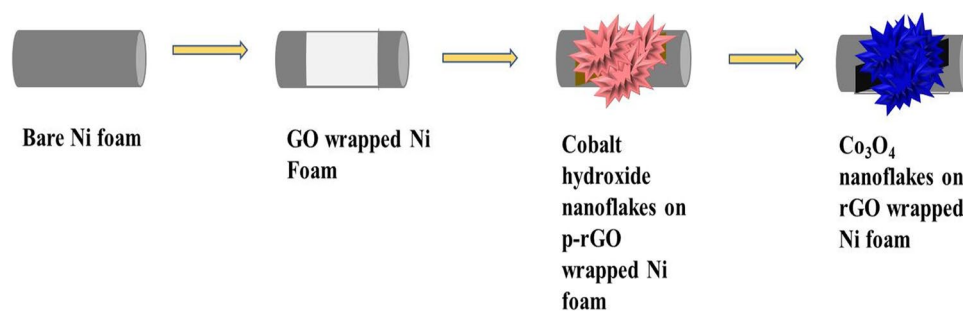
The flake graphite or graphite powder/sodium nitrate combination was produced at a weight ratio of 2:1. At 15 °C, the sample was stirred into a beaker with 98 wt.%. Sulfuric acid and suspended material were formed, in this beaker, which has been placed in the ice bath. After that, KMnO_4 powder, which also behaved as an oxidation agent, was slowly added to the mixture while it was being stirred constantly. The weight of the KMnO_4 powder is three times more than the weight of the mixed substance. The temperature of the solution should be kept below 20 °C for 2 h, and the solution should be agitated constantly throughout this time period. To finish dissolving the KMnO_4 , the temperature was maintained at 35 °C for 30 min. Because a significant quantity of heat was produced when concentrated H_2SO_4 was diluted, a specific amount of deionized water was added to the mixture. The mixture was constantly stirred for 15 min, after which specific quantities of heated water and 30% H_2O_2 aqueous were added in various proportions. When the brilliant yellow coloration was still warm, the combination was filtered using Whatman filter paper, which resulted in the filtering of the suspended material, as well as the liquid portion, which was distilled water and dried in a vacuum oven at 70 °C for 24 h [35–41].

3 Reduced graphene oxide/transition metal oxide composite electrodes

3.1 rGO/metal oxide composites

Many researches on composite materials combining transition metal oxide nanoparticles and graphene has been published in recent years, and they have shown excellent electrochemical energy storage capability. It was discovered that some scientists utilized chemical methods to synthesize monometallic oxide and graphene in advance, then mixed them using mechanical stirring or high-temperature calcination to form composite materials. Jinhui Xua et al. demonstrated the fabrication of NiO/rGO composites using nickel nitrate, urea, and graphene oxide as raw materials

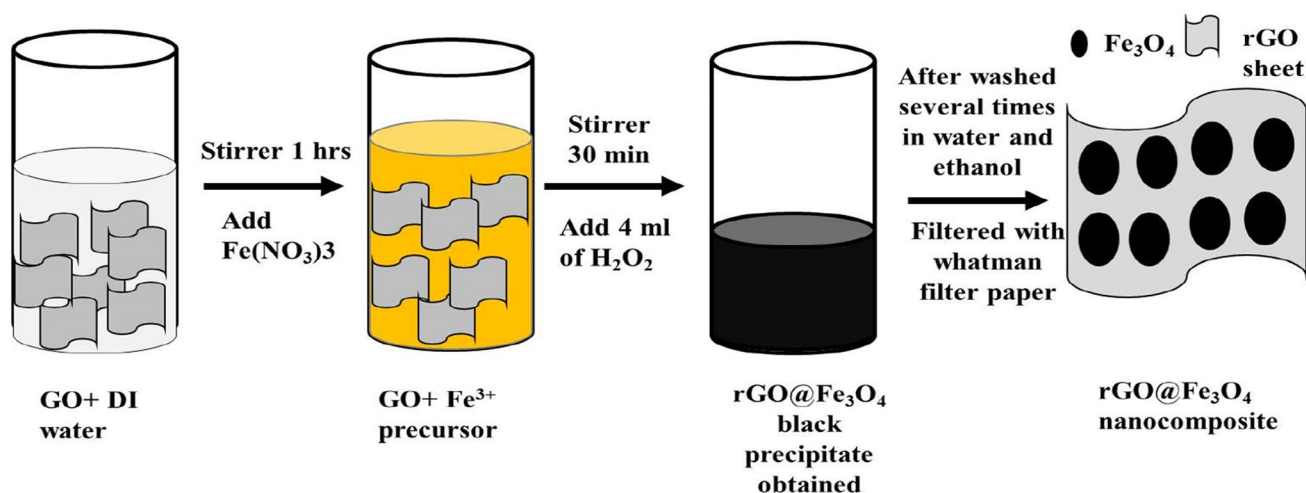
Scheme 1 The synthesis of Co_3O_4 nanoflakes on rGO-wrapped Ni foam is depicted schematically [44]



in a hydrothermal reduction precursor calcination method. Chemical research showed that the specific capacitance of the NiO/rGO composite was achieved at 171.3F/g in a 6-mol/L KOH electrolyte with a current density of 0.5A/g after graphene oxide was reduced to graphene and NiO nanoparticles were placed between layers of graphene. After 2000 cycles of galvanostatic current charge and discharge at 5-A/g current density, the composite material's average specific capacitance dropped by 20.93%. In the composite material, NiO nanoparticles are more uniformly embedded in the graphene layer. These composite materials' three-dimensional layered structure improves the performance of supercapacitor applications. The author has done only in low-temperature synthesis due to that percentage of evaluation is reduced in material [42]. Yuanyuan Zhu et al. reported that the $\alpha\text{-Fe}_2\text{O}_3/\text{rGO}$ composite is a viable candidate material as a negative electrode in asymmetric aqueous supercapacitors. To create $\alpha\text{-Fe}_2\text{O}_3/\text{rGO}$, a simple hydrothermal method with surface potential change was employed. Because the energy storage behavior of $\alpha\text{-Fe}_2\text{O}_3$ is unknown, it is reasonable to infer that $\alpha\text{-Fe}_2\text{O}_3$ participates in the energy storage process through the Faradaic reaction. $\alpha\text{-Fe}_2\text{O}_3/\text{rGO}$ composites were used as anode materials for supercapacitors, and they showed good electrochemical performance with a high specific capacitance of 255 F g^{-1} at 0.5 A g^{-1} , excellent rate capability, and good cycling life in a 1-M Na_2SO_4 aqueous electrolyte with a wide potential window (1.2 V). After 11,000 cycles of galvanostatic charge discharge (GCD) testing, there is only about 10% loss. Finally, due to strong faradaic reaction of $\text{Fe}_2\text{O}_3/\text{rGO}$ composite sample is suitable for electrode material for asymmetric supercapacitors. The low amount of $\alpha\text{-Fe}_2\text{O}_3$ is mixed with rGO; this may be attributed to low specific capacitance of the device [43]. Shipra Raj et al. developed a novel ammonia evaporation technique (AET) followed by a heat treatment strategy for in situ conversion of GO to rGO on Ni foam (NF) during Co_3O_4 deposition. The likely mechanisms of the reaction, as well as the technique of synthesis, are shown schematically in Scheme 1. The material is well-supported by the rGO-wrapped Ni foam, which provides mechanical stability and also simplifies assembly. Charge transfer from metal oxide to metal current beneath its collector.

This structure exhibited supercapacitor characteristics, with a substantially greater specific capacity of 1328 C g^{-1} at 2-A g^{-1} current density and excellent stability. Electrochemical samples were analyzed in a two-electrode system with rGO- $\text{Co}_3\text{O}_4/\text{NF}$ or $\text{Co}_3\text{O}_4/\text{NF}$ electrodes as positive electrodes and activated carbon/NF electrodes as negative electrodes to test the practical application of materials as supercapacitors, and were defined as RCO/AC and CO/AC, respectively. The $\text{Co}_3\text{O}_4\text{-rGO}/\text{NF}/\text{AC}$ asymmetric design also obtained a high energy density of 20 Wh kg^{-1} at a power density of 1200 W kg^{-1} . These were accomplished for a $\text{Co}_3\text{O}_4\text{-rGO}/\text{Ni}$ foam-based asymmetric device, indicating the material as a potential candidate for supercapacitor applications. The three-dimensional structure electrodes facilitate ionic diffusion throughout the charging-discharging process, resulting in a very high specific capacitance and power density [44]. N.A. Devi et al. reported on the production of $\text{Fe}_3\text{O}_4/\text{rGO}$ nanocomposite, which was accomplished via a straight-forward chemical reduction procedure. The production of $\text{Fe}_3\text{O}_4/\text{rGO}$ nanocomposite is shown in Scheme 2 using a step-by-step diagram. Fe_3O_4 nanoparticles with particle sizes range from 100 to 250 nm. The 10-mM, 15-mM, 20-mM, and 25-mM $\text{Fe}_3\text{O}_4/\text{rGO}$ nanocomposites are made using the same procedure. The 10-mM, 15-mM, 20-mM, and 25-mM Fe precursors are used in the sample preparation. The study employed Fe_3O_4 nanoparticles with sizes ranging from 100 to 250 nm for their study. For a 25-mM $\text{Fe}_3\text{O}_4/\text{rGO}$ nanocomposite, a maximum specific capacitance of 416 F/g has been obtained. Finally, after 1000 cycles, the 25-mM $\text{Fe}_3\text{O}_4/\text{rGO}$ nanocomposite has a cycling stability of 88.57% at 5 A g^{-1} . When compared to other ratios of precursor material, the high concentration of iron precursors decorated in rGO nanosheet has the greatest performance for supercapacitor applications [45].

Ghasemi et al. prepared for the first time MnO_2/GO nanohybrids that were synthesized using an electrostatic precipitation process. $\text{MnO}_2/\text{RGO}/\text{SS}$ has high power and energy densities of 52.1 Wh kg^{-1} and 625.0 Wh kg^{-1} at 1 A g^{-1} , respectively. Furthermore, after 500 cycles at 200 mV s^{-1} , roughly 93% of the original capacitance was maintained, giving the nanohybrid a good material as an active material for supercapacitors. Experimental evidence



Scheme 2 Synthesis of $\text{Fe}_3\text{O}_4/\text{rGO}$ nanocomposite [45]

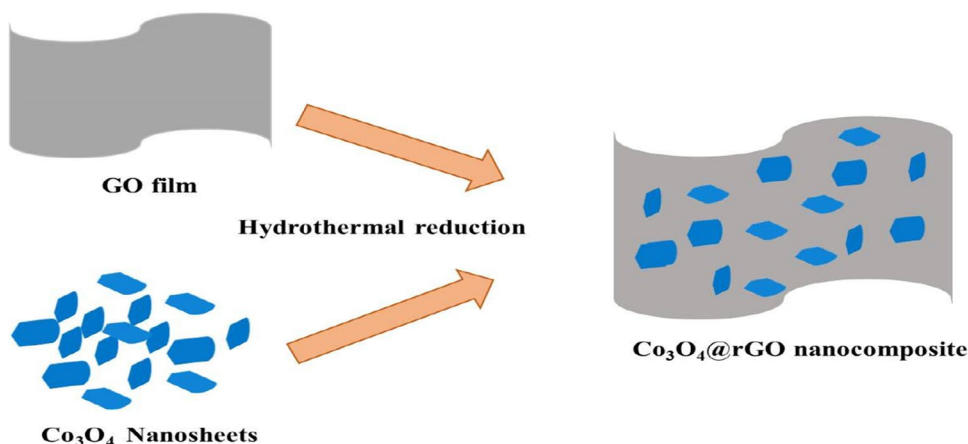
indicates that this structure may provide a suitable interface for cation exchange and charge storage when subjected to electrochemical experiments. The author tested only with stainless steel conductor electrode for supercapacitor application [46]. Y. N. Sudhakar et al. reported ultrasonically prepared copper oxide (CuO) nanoparticles and rGO-CuO nanocomposites. For the first time in history, reduced graphene oxide has been synthesized using piperine produced from *Piper nigrum*, which is a green reducing agent. This method was utilized to fabricate rGO-CuO nanocomposites in a variety of ratios, including 1:3, 1:2, 1:1, 2:1, 3:1, 4:1, 5:1, and 6:1, even in a variety of sizes. When compared to rGO and CuO electrodes, the rGO-CuO nanocomposite with composition (3:1) had lower resistance and higher specific capacitance. As a result, a 3:1 rGO-CuO nanocomposite electrode has been evaluated in four different electrolytes at 0.1 M concentrations, including Na_2SO_4 , H_3PO_4 , H_2SO_4 , and $\text{H}_2\text{SO}_4:\text{H}_3\text{PO}_4$ (9:1). According to electrolyte studies, the acid combination (9:1) is suitable for use in supercapacitor applications. The highest value of specific capacitance achieved was 224 F g^{-1} at 5 mV s^{-1} in the ratio of rGO-CuO (3:1). The maximal energy density was 14 Wh kg^{-1} and the maximum power density was 12 kW kg^{-1} . The nanoleaf CuO high surface area acts as an excellent support for the rGO , improving the electrochemical process and resulting in increased capacitance [47].

Yingtao Zhang et al. synthesized that a simple one-step hydrothermal process is used to make ultrafine SnO_2 nanorods/ rGO composites. We discovered that, in general, when rGO is coated with SnO_2 nanorods, the average size of the nanorods increases, but the size of the crystals is minimal. When hydrochloric acid is added to the SnO_2 nanorods/ rGO (1:2) water dispersion for further hydrothermal treatment at elevated temperatures, the smaller SnO_2

particles act as a source of Sn, enabling the larger SnO_2 particles to continue to improve. The average size of SnO_2 nanorods in the final material grew, and SnO_2 crystallinity improved. The electrochemical performance of the resulting composite electrode is enhanced, with a specific capacitance of 262.2 F g^{-1} at a current density of 100 mA g^{-1} in 1 M Na_2SO_4 . In this manuscript author explains that the SnO_2 nanorods are equally distributed on rGO nanosheet and the ultrafine SnO_2 nanorods/ rGO composite materials are produced by subsequently treated with secondary hydrothermal technique using HCl and KMnO_4 [48]. Feng Du et al. produced porous Co_3O_4 nanosheets @ RGO nanocomposite using a simple hydrothermal reduction method. As illustrated in Scheme 3, the interaction of the $-\text{OH}$ and $-\text{COOH}$ functional groups of GO films with the surface of Co_3O_4 nanosheets is expected to be effective for the formation of a $\text{Co}_3\text{O}_4@\text{RGO}$ nanocomposite. They have deduced that now the two samples (Co_3O_4 and $\text{Co}_3\text{O}_4@\text{RGO}$ nanocomposite) will perform differently as electrode materials in supercapacitors because of their distinct structure. The porous Co_3O_4 nanosheets in the $\text{Co}_3\text{O}_4@\text{RGO}$ nanocomposite have a higher specific surface area, which is advantageous for providing additional electrochemical reaction regions. While exposed to 3000 cycles, both electrodes showed outstanding extended cycle life, especially the $\text{Co}_3\text{O}_4@\text{RGO}$ nanocomposite electrode, whose capacitance decreased by just 4.7% of its initial capacitance throughout the experiment [49].

J. Jayachandran et al. published a comprehensive study on the fabrication of rGO/ZnO composites utilizing a simple precipitation technique and an ultrasonic aided solution approach. The incorporation of spherical-shaped ZnO nanoparticles into the electrode material seems to have the potential to produce an electrode material with a high specific surface area. The specific capacitance performance of the

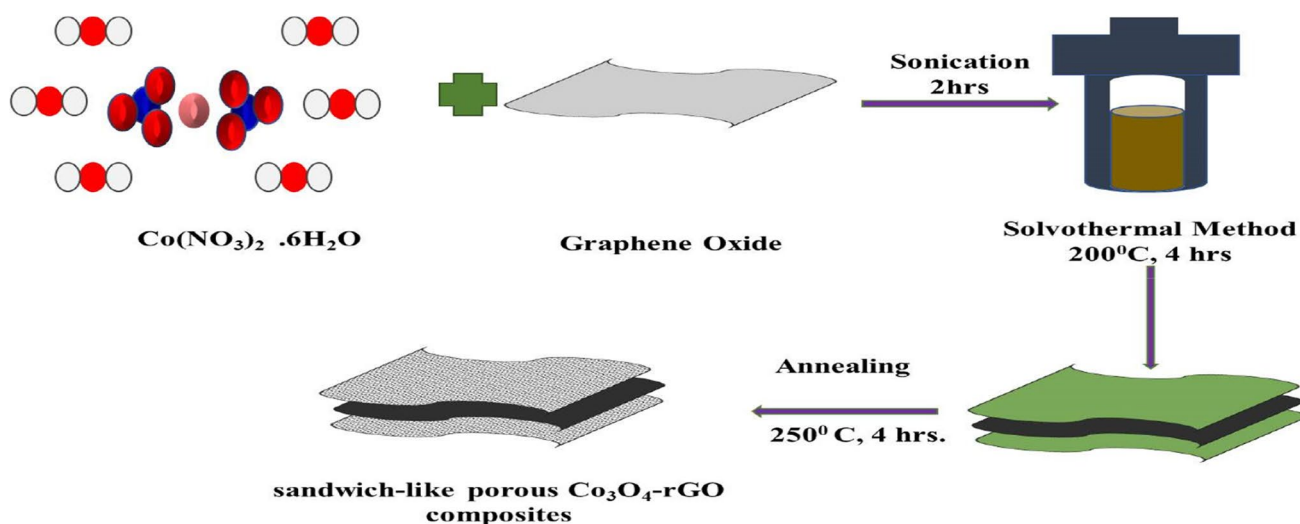
Scheme 3 Schematic diagram of synthesized Co_3O_4 nanosheets @RGO nanocomposite [49]



rGO/ZnO composite is significantly affected by the shape of the composite. The specific capacitance of the ZnO and rGO/ZnO composite electrodes was evaluated at a reduced scan rate of 5 mV s^{-1} and was found to be 199 and 312 F g^{-1} , respectively, at the lower scan rate. The produced rGO/ZnO composite electrode's long-term cycling stability is investigated using a 1000 cycle CV analysis at a scan rate of 10 mV s^{-1} [26]. C. Lai et al. prepared by a solvothermal approach has been used to design a novel hierarchical sandwich-like porous nanostructure of Co_3O_4 -rGO composites. $\text{Co}(\text{OH})_2$ nanosheets with hierarchical porous structures were produced on the double surfaces of rGO nanosheets, resembling sandwich-like structures. Following that, the $\text{Co}(\text{OH})_2$ -rGO composites were heated for 2 h at 250°C to form the porous Co_3O_4 -rGO sandwich-like structure shown in Scheme 4 during the heat treatment. They extensively investigated the electrochemical properties of the electrode of Co_3O_4 -rGO composites in a three-electrode cell configuration using cyclic voltammetric (CV)

and galvanostatic charge–discharge (GCD) in 6 M of KOH solution. At a current density of 0.5 A g^{-1} , the sandwich-like porous Co_3O_4 -rGO achieved high specific capacitance value of 1260.6 F g^{-1} and a power density of 400 W kg^{-1} , the energy density is 38.8 Wh kg^{-1} , and the cycle life is outstanding, with 88.0% of the initial capacitance after 10,000 cycles. The sandwich-like porous composites were generated in this outcome of the literature by using the solvothermal approach. The two-dimensional porous structure has high surface area and strong cyclic stability [50].

Y. Chen et al. prepared the ruthenium oxide nanodots have been formed on reduced graphene oxide (RGO) sheets homogeneously by hydrothermal and annealing techniques. A sol–gel synthesis method is used to produce RGO/ruthenium oxide composites, which seems primarily determined by hydrothermal and annealing treatments using GO and hydrous ruthenium chloride as precursor materials. To be more specific, GO was produced using a modified version of the Hummers' technique. This technique has been improved,



Scheme 4 The hierarchical sandwich-like porous Co_3O_4 -rGO composites' production pathway [50]

and a maximum of 471 F g^{-1} has been obtained in composites loaded with 45 wt.% RuO_2 at 0.5 A g^{-1} . Their specific capacitance maintains 92% of the maximal capacitance after 3000 cycles. The homogeneity of RuO_2 on RGO as well as the interactive effects between them are credited with the excellent integrated capacitive properties of the material [51]. A. Viswanathan et al. created the $\text{rGO}/\text{V}_2\text{O}_5$ nanocomposite in a single step of chemical synthesis. The mass ratios of the rGO and V_2O_5 are 7.69% and 92.31%, respectively, in the overall mixture. It is important to transform V^{5+} to V^{4+} and conversely, in order to complete the redox conversion of V_2O_5 . The quantity of energy stored is similarly directly proportional to the size of the potential window applied. At lower current densities, the electrode material loses less potential due to its intrinsic resistance, enabling more energy storage. The storage parameters (specific capacitance, specific capacity, energy density, power density, and columbic efficiency) that were derived from a linear discharge approach were a high specific capacitance (120.62 F g^{-1}), a high specific capacity (144.74 C g^{-1}), an energy density (24.12 W h g^{-1}), a power density ($2.647 \text{ kW k g}^{-1}$), and a current density of 2 A g^{-1} . After being tested for 5000 cycles, the nanocomposite maintained 100% of its original capacitance. Also, after 10,600 cycles at a potential scan rate of 400 mV s^{-1} , the capacitor maintained 38% of its original capacitance. The V_2O_5 nanoparticles are equally dispersed on rGO surface. So the electrode material was able to reach the excellent cyclic stability and high energy density (Table 1) [52].

3.2 rGO/binary metal oxide composites

A composite metal oxide is a combination of two distinct metal oxides that have a different chemical composition. Reduced graphene oxide and metal oxide serve as electrode materials in supercapacitor applications. The researchers that worked on the bimetallic oxide/ rGO composite material had the best results in electrochemical tests. The following studies are the outcome of the researchers' work [53].

Nirmallesh Naveen et al. demonstrated that by synthesizing the combustion method and using urea as the fuel source, the $\text{NiCo}_2\text{O}_4/\text{rGO}$ composite was converted into a functional electrode. $\text{NiCo}_2\text{O}_4/\text{rGO}$ composites fabricated with mesoporous structured NiCo_2O_4 are projected to increase the capacitive performance of $\text{NiCo}_2\text{O}_4/\text{rGO}$ composites by enriching the synergistic combination of rGO and NiCo_2O_4 . The electrochemical evaluation of the electrode materials showed the presence of faradaic activity in the materials. The $\text{NiCo}_2\text{O}_4/\text{rGO}$ composite had a high specific capacity of 662.3 C g^{-1} at 5 mVs^{-1} in 1 M KOH aqueous electrolyte. $\text{NiCo}_2\text{O}_4/\text{rGO}$ maintained more capacitance; at the end of 2000 cycles, 94% of the original capacitance was retained at a current density of 3 Ag^{-1} . The charge/discharge process

has a long cycle life owing to the exceptional mechanical strength of RGO in NiCo_2O_4 [54]. M.B. Askari et al. studied the hydrothermal synthesis of an asymmetric supercapacitor electrode material with $\text{NiFe}_2\text{O}_4/\text{rGO}$ and placement on the surface of the glassy carbon electrode (GCE) for supercapacitor studies. Similarly, NiFe_2O_4 performs as an electro active material that sits between rGO layers and improves charge storage. There is a huge amount of oxygen and oxygen-containing groups in graphene oxide. Negatively charged oxygen absorbs Fe^{+3} and Ni^{+2} cations, forming NiFe_2O_4 on the rGO surface. The presence of NiFe_2O_4 on the surface of rGO increases the electrical conductivity while also creating new conducting pathways for charge transfer, resulting in a higher specific capacitance than when the rGO is not present in the electrode structure. When compared to pure NiFe_2O_4 nanoparticles and $\text{NiFe}_2\text{O}_4/\text{rGO}$ nanocomposite, rGO displays the electrochemical double-layer capacitor mechanism for charge storage, and its specific capacity is comparatively small. At a scan rate of 10 mV/s , $\text{NiFe}_2\text{O}_4/\text{rGO}$ obtains a capacitance of 584.63 F/g that becomes three times greater than pure NiFe_2O_4 . Moreover, as compared to NiFe_2O_4 , the $\text{NiFe}_2\text{O}_4/\text{rGO}$ electrode has a greater rate capability and cycling stability. After 2000 charging/discharging cycles, the $\text{NiFe}_2\text{O}_4/\text{rGO}$ retains 91% of its capacitance [55]. F. Meng et al. synthesized $\text{NiCo}_2\text{O}_4/\text{rGO}$ through a hydrothermal procedure followed by a spray drying process. The spray drying method has decreased the evaporation time in the electrode fabrication process. The specific capacitance of $\text{NiCo}_2\text{O}_4/\text{rGO}$, which becomes 702 F g^{-1} at 0.5 A g^{-1} , is almost 2.6 times that of a pure NiCo_2O_4 electrode. The rGO sheets are very essential in composite materials. A symmetric two-electrode ($\text{NiCo}_2\text{O}_4/\text{rGO}/\text{NiCo}_2\text{O}_4/\text{rGO}$) electrode materials with 1-M KOH aqueous electrolyte were also fabricated to test the performance of $\text{NiCo}_2\text{O}_4/\text{rGO}$ for practical applications. The two-electrode system has a specific capacitance of 259 Fg^{-1} at a current density of 0.5 Ag^{-1} [56].

Z. Wang et al. used a mild technique to make $\text{rGO}/\text{NiMn}_2\text{O}_4$ composites of rGO and NiMn_2O_4 nanorods produced by co-precipitation in an ethanol–water solution. In three-electrode systems, the electrochemical performance of $\text{rGO}/\text{NiMn}_2\text{O}_4$ nanorod composite potential window is $0\text{--}0.9 \text{ V}$ at $1\text{-M Na}_2\text{SO}_4$ aqueous electrolyte. The rGO represents a key function in improving the specific capacitance and cyclic stability of the composite material. At a current density of 1 A g^{-1} , the hybrid material has the maximum specific capacitance of 693 F g^{-1} . The capacitance of hybrid material maintains 91.38% of the initial capacitance after 2000 charging/discharging cycles, demonstrating good electrochemical stability. The electrode material of the one-dimensional nanorod is embedded in the two-dimensional rGO surface. As a result, this composite material has a high capacitance and a high degree of stability due to the structure of the material [57]. Ting Liu et al. demonstrated

Table 1 Comparison of different metal oxide/rGO composite material performance

Electrode material	Electrolyte	Specific capacitance	Energy density	Power density	Capacity retention	Ref
CuO/RGO	0.5 M K ₂ SO ₄	326 F g ⁻¹ at 0.5 A g ⁻¹	65.7 Wh kg ⁻¹	302 W kg ⁻¹	1500 cycles at 5 A g ⁻¹	[75]
Nanoflakes MnO ₂ /rGO	1 M Na ₂ SO ₄	140.3 F g ⁻¹ at 1 mA	19.5 Wh kg ⁻¹	633.7 W kg ⁻¹	5000 cycles at 2 mA 99.4%	[76]
rGO@ NiO composites	6 M KOH	1093 F g ⁻¹ at 1 A g ⁻¹	-	-	90.6% 5000 cycles	[77]
Layered NiO/RGO	6 M KOH	782 F g ⁻¹ at 0.5 A g ⁻¹	32.5 Wh kg ⁻¹	375 W kg ⁻¹	94.1% retention at 2 A g ⁻¹ after 3000 cycles	[78]
Co ₃ O ₄ /RGO composite	3 M KOH	340 F g ⁻¹ at 1 A g ⁻¹	-	-	50 cycles retention of about 85%	[79]
Mn ₃ O ₄ nanoflakes/rGO	1 M Na ₂ SO ₄	351 F g ⁻¹ at 0.5 A g ⁻¹	-	-	80.1% of capacitance after 10,000 cycles	[80]
RGO-Fe ₃ O ₄	1 M KOH	315 C g ⁻¹ at 5 A g ⁻¹	-	-	95% retention after 2000 cycles	[81]
RGO/Cu ₂ O	1 M KOH	98.5 F g ⁻¹ at 1 A g ⁻¹	-	-	1000 continuous charg- ing/discharging	[82]
CoO/rGO	2 M KOH	1615 F g ⁻¹ at a 1 A g ⁻¹	62.46 Wh k g ⁻¹	1600 W k g ⁻¹	88.12% retention after 15,000 cycles at 5 A g ⁻¹	[83]
rGO/TiO ₂	1 M H ₂ SO ₄	233.67 F g ⁻¹ at 1 A g ⁻¹	32.454 Wh k g ⁻¹	716.779 W k g ⁻¹	98.2% even after 2000 cycles	[84]
Fe ₂ O ₃ /rGO	3 M KOH	106.2 F cm ⁻³ at 1 mV s ⁻¹	0.056 Wh cm ⁻³	6.21 W cm ⁻³	-	[85]
CuO/rGO	1 M Na ₂ SO ₄	80 F g ⁻¹ at 2 A g ⁻¹	-	-	-	[86]
rGO/TiO ₂ nanosheets	1 M Na ₂ SO ₄	1565 F/g at 3 A/g	15.5 Wh/kg	1.1 kW/kg	87% even after 1000 cycles	[87]
Mn ₃ O ₄ /rGO	1 M Na ₂ SO ₄	342.5 F g ⁻¹ at of 1 A g ⁻¹	27.41 Wh kg ⁻¹	8 kW kg ⁻¹	85.47% capacitance retention under 10,000 cycles	[88]
Co ₃ O ₄ -rGO	6 M KOH	636 F g ⁻¹	35.7 Wh kg ⁻¹	225 W kg ⁻¹	Capacitance retention of 95% after 1000 cycles	[89]
rGO-TiO ₂	1 M Na ₂ SO ₄	225 F g ⁻¹ at 0.125 A g ⁻¹	-	-	86.5% of capacitance after 2000 cycles	[90]
RGO/V ₂ O ₅	1 M Na ₂ SO ₄	218.4 F/g at 10 mV/s	-	2.201 kW/kg	-	[91]
V ₂ O ₅ -rGO	1 M LiClO ₄ /PC	511.7 mF cm ⁻²	13.3 W h kg ⁻¹	625 W kg ⁻¹	-	[92]
Pd/rGO	1 M KOH	1524.7 F/g at 20 mV/s	-	-	92.1% capacitance retention after 2000 cycles	[93]
rGO@Co ₃ O ₄	0.1 M KOH	276.1 F g ⁻¹ (5 mV s ⁻¹)	-	-	82.37% capacitance retention after 10,000 cycles	[94]
ZnO@rGO	0.1 M KOH	102.4 F/g at 30 mV/s	-	-	82.5% for 3000 cycles	[95]
Ni(OH) ₂ -ErGO	1 M KOH	3138 F/g at 20 mV/s	-	-	Capacitance retention of 88.6% after 3000 cycles	[96]
Fe ₃ O ₄ /rGO	2.0 M KOH	455 F g ⁻¹ at 8 mV s ⁻¹	-	-	Retention ratio of 91.4 after ~ 190 cycles	[97]
Co ₃ O ₄ @CG	30 wt.% KOH	600 F/g at 0.7A/g	-	-	Retained 94.5% of its initial capacitance even after 5000 cycles	[98]
G wrapped Co ₃ O ₄	0.5 M BMIM-BF ₄ / CH ₃ CN	710 F g ⁻¹ at 5 mV s ⁻¹	52.84 Wh/kg	986.32 W/kg	Stable cyclic perfor- mance over 10,000 charge–discharge cycles	[99]

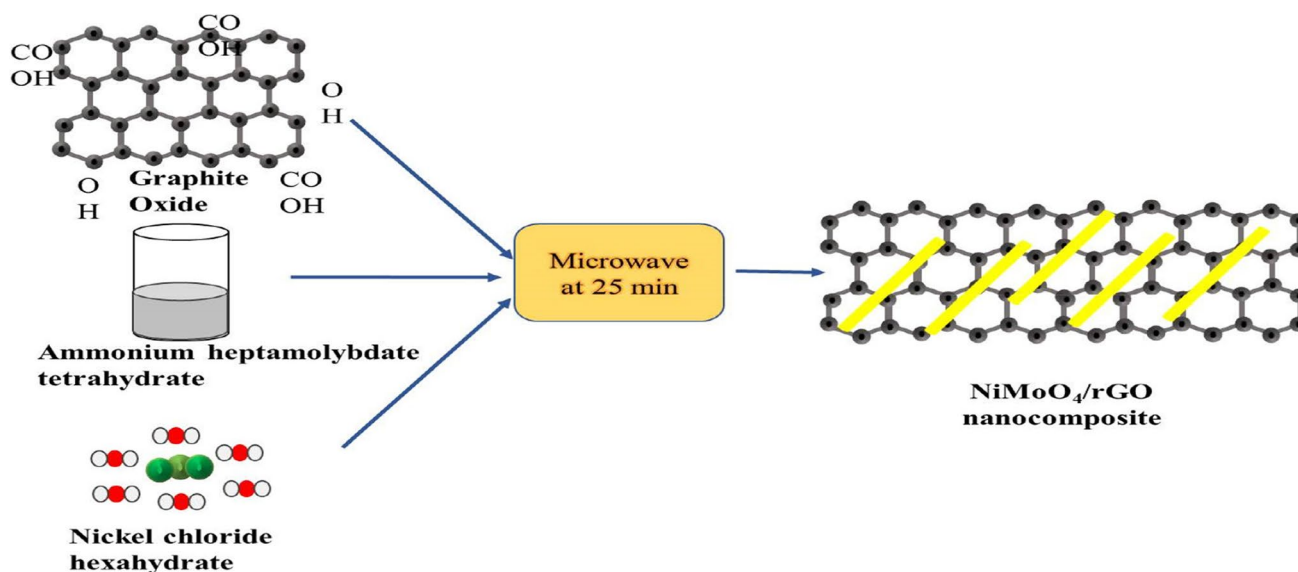
Table 1 (continued)

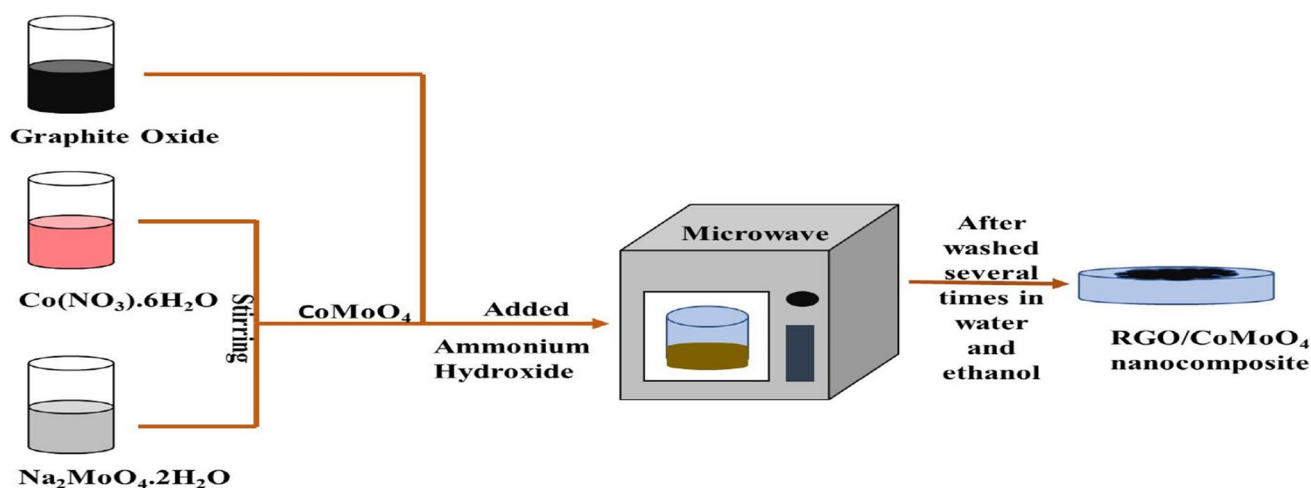
Electrode material	Electrolyte	Specific capacitance	Energy density	Power density	Capacity retention	Ref
G wrapped NiO	5 M KOH	549 F g ⁻¹ at 10 mV s ⁻¹	-	-	Over 88% of the initial capacitance after 2500 cycles	[100]
Mn ₃ O ₄ -Fe ₂ O ₃ /Fe ₃ O ₄ @rGO	1.0 M KOH	590.7 F/g at 5 mV/s	-	-	64.5% after 1000 cycles	[101]
NiO-MnO ₂ @rGO	0.1 M KOH	165.7 mAh/g at 20 mV/s	-	-	83.2% after 2000 continuous cycles	[102]

that the NiMoO₄/rGO nanocomposite was synthesized by a microwave-solvothermal method shown below in Scheme 5. The GO was changed to rGO using the Hummer's technique, and the bulk of the oxygen groups were removed during the microwave heating step, which was performed in the laboratory. Ni²⁺ and MoO₄²⁻ ions preferentially bonded to functional groups to create NiMoO₄ nanorods around the same time. The performance of the pure NiMoO₄ and NiMoO₄-rGO nanocomposite was tested with three-electrode configuration systems. The specific capacitance of the pure and nanocomposite was 800 F g⁻¹ and 1274 Fg⁻¹ at current density of 1 Ag⁻¹, respectively. After 1000 charging/discharging cycles, the capacitance retention is 81.1%. The asymmetrical supercapacitor was built with mesoporous NiMoO₄-rGO as the positive electrode and NG as the negative electrode. The specific capacitance of the asymmetrical-supercapacitor is 295 F g⁻¹ at 1 A g⁻¹ in a potential window of -1 to 0 V, and both the cyclic voltammetry and galvanostatic charging/discharging curves are negative [58].

Xu et al. enhanced the electrochemical performance of the RGO/CoMoO₄ nanocomposite produced using the

microwave irradiation aided technique shown in Scheme 6. Moreover, CoMoO₄ nanoparticles on graphene sheets in RGO/CoMoO₄ composites should lead to improved electrochemical performance due to an increase in surface area and active sites. The surface of RGO has a strong attachment of CoMoO₄ particles. As for the pure CoMoO₄ and RGO/CoMoO₄ tested with three-electrode systems, the RGO/CoMoO₄ nanocomposite was able to achieve the highest specific capacitance compared to pure CoMoO₄ at 5 mVs⁻¹. The produced RGO/CoMoO₄ composites were annealed at 500 °C for 5 h in an N₂ environment to evaluate the impact of the crystalline phase on the electrochemical performance of RGO/CoMoO₄. After the annealed process, the RGO/CoMoO₄ nanocomposite specific capacitance suddenly decreases from 322.5 to 102.5 F g⁻¹ at 5 mV s⁻¹ [59]. Yuan et al. investigated the electrochemical performance of MnCo₂O₄@ reduced graphene oxide as a supercapacitor electrode material. The MnCo₂O₄@rGO composite was produced using a one-step hydrothermal method, and the crystal size of the composite was measured using XRD analysis to determine its crystal size. Because of its

**Scheme 5** Synthesis route of NiMoO₄/rGO nanocomposite [58]



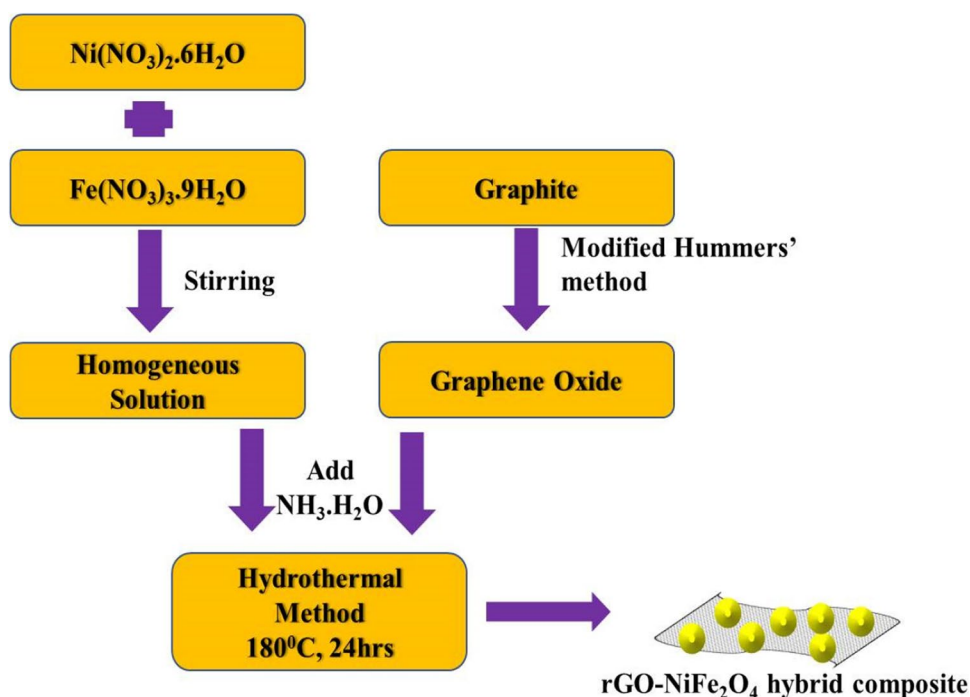
Scheme 6 Prepared method of RGO/CoMoO₄ nanocomposite [59]

superior conductivity and chemical durability, graphene can be employed as an appropriate carrier to load nanoparticles for the construction of new types of electrode materials. The capacitive behavior of MnCo₂O₄@rGO was superior to that of pure MnCo₂O₄. The cause of the increase in pure to composite capacitance, as well as rGO, was due to supercapacitor applications. The MnCo₂O₄@rGO nanocomposites displayed high specific capacitance of 334 F g⁻¹ at 1 A g⁻¹ and outstanding cycle stability of 98% after 2000 cycles [60].

Ping He et al. created the reduced graphene oxide-CoFe₂O₄ composite using a hydrothermal method using sodium borohydride as the reduction agent. A modified Hummers methodology was used to create graphene oxide. The electrode material samples GO, RGO, CoFe₂O₄, GO-CoFe₂O₄, and RGO-CoFe₂O₄ were synthesized as noted and Cs of RGO (89.9 F g⁻¹), GO-CoFe₂O₄ (21.1 F g⁻¹), CoFe₂O₄ (18.7 F g⁻¹), and RGO-CoFe₂O₄ (123.2 F g⁻¹) at the current density of 5 mA cm⁻². The RGO-CoFe₂O₄ composite has a high specific capacitance in this electrochemical investigation when compared to other materials. In this article the synthesized material has large particle size and low surface area because this attributes to low performance of application [61]. A. Juliet Christina Mary et al. synthesized the ZnCo₂O₄/rGO nanocomposite as an electrode material for supercapacitor applications. The hydrothermal synthesis method used in the ZnCo₂O₄/rGO nanocomposite production utilizes basic techniques to complete the operation. Depending on the particular capacitances they contain, the three synthesized samples, rGO, ZnCo₂O₄, and ZnCo₂O₄/rGO nanocomposite, exhibit a wide variety of behavior when it comes to electrochemical performance. At a current density of 0.75 A/g, the ZnCo₂O₄/rGO nanocomposite had a high specific capacitance of 704.2 F/g. Because of high specific capacitance value, it is suitable for positive electrode material in

asymmetric supercapacitors [62]. M. Isacfranklin et al. reported that the sea urchin-like NiCo₂O₄/rGO composite was produced by the solvothermal method. A pure Co₃O₄ electrode material has been synthesized, as well as binary NiCo₂O₄ and NiCo₂O₄/rGO nanocomposite electrode materials, for use in energy storage supercapacitor applications that are environmentally friendly. By using solvothermal synthesis methods, the NiCo₂O₄/rGO composite was able to achieve an excellent shape and a large surface area. This kind of sea-urchin-like electrode enhances the electrochemistry efficiency of the insertion/extraction process by allowing for fast electron ion transit during the insertion/extraction reaction. As a result, sea-urchin-like NiCo₂O₄/rGO structures are recommended as an appropriate electrode material for long-term energy storage. The urchin-like NiCo₂O₄/rGO got a good specific capacitance and excellent cycle stability, with a value of 672.79 F/g at 10 mV/s [63]. Y-Z Cai et al. prepared a reduced graphene oxide/NiFe₂O₄ nanohybrid electrode material for supercapacitor applications. For the production of this composite of NiFe₂O₄ and rGO in the 3:7 ratio indicated in Scheme 7, the hydrothermal method would be used. Nickel and iron ions in the solution are transformed into nickel-iron oxide nanoparticles by graphene oxide sheets that have chemically adsorbed to the surface of the solution. When pure NiFe₂O₄ and NiFe₂O₄/rGO composites were the three-electrode systems in 1-M Na₂SO₄ aqueous electrolyte, they reached a specific capacitance of 50 F g⁻¹ at a current density of 0.5 A g⁻¹ and a specific capacitance of 215.7 F g⁻¹ at a current density of 0.5 A g⁻¹. As a consequence, rGO has contributed to the improvement of composite materials as compared to pure materials [64]. C. Zhang et al. justified the NiCo₂O₄@rGO hybrid material as a high-performance electrochemical electrode material. A novel method of dipping and drying was used

Scheme 7 Preparation of reduced graphene oxide/ NiFe_2O_4 nanohybrid electrode material [64]



to create the hybrid $\text{NiCo}_2\text{O}_4@\text{rGO}$ material. The three-electrode materials evaluated in electrochemical performance, rGO, NiCo_2O_4 , and $\text{NiCo}_2\text{O}_4@\text{rGO}$, each have a working electrode, a counter electrode of Pt foil, and a reference electrode of a standard calomel electrode (SCE). The materials used here, in combination with the unique electrical properties of the $\text{NiCo}_2\text{O}_4@\text{rGO}$ hybrid nanostructure, demonstrate the immense potential of electrode materials for supercapacitors [65]. Gao et al. produced a $\text{ZnCo}_2\text{O}_4\text{-rGO}$ composite with intertwined sheets grown onto a nickel foam substrate via a simple hydrothermal deposition and thermal processing, which can be directly used as a binder-free electrode for a supercapacitor. It is possible to construct a porous $\text{ZnCo}_2\text{O}_4\text{-rGO}$ composite composed of interconnected mesoporous sheets with vertical macroporous channels by connecting the mesoporous sheets with vertical macroporous channels. The vertical macroporous channels allow electrolyte to be injected into deep inner cavities of the porous electrode, thereby facilitating access to the innermost area of the electrode. The Cs in the $\text{ZnCo}_2\text{O}_4\text{-rGO}$ electrode decays gradually from an initial Cs reading of 1875 to a final Cs reading of 1155 F g^{-1} . As a result, the 65% initial Cs ratio indicates moderate cyclability. The high Cs and restricted potential range of the $\text{ZnCo}_2\text{O}_4\text{-rGO}$ electrode mean that asymmetric devices are an attractive method for extending the potential window of supercapacitors and, as a result, increasing their E_{cell} . Depending on the outcomes of these electrochemical experiments, the $\text{ZnCo}_2\text{O}_4\text{-rGO/AC}$ ASC described herein

is considered to be an efficient supercapacitor with a long lifetime (Table 2) [66].

3.3 rGO/ternary metal oxide composites

The TMO nanocomposite has a large surface area and good cycle stability of electrochemical performance, and when combined with the RGO composite, the researchers were able to achieve the amazing results they demonstrated. The researchers had a major role in the development of the RGO/ternary transition metal oxide-based electrode material used in supercapacitor application that was created. It is possible to accomplish the basic advantages of RGO/ternary metal oxides via strong electrical conductivity, an abundance of electroactive centers, uniform distribution, and eco-friendliness, among other characteristics [67, 68].

Wu et al. investigated the $\text{Co}_3\text{O}_4/\text{NiO/rGO}$ hybrid composite ternary composites prepared through the hydrothermal method in relation to the cobalt–nickel molar ratio, calcination temperature, and the amount of rGO added. Next, $\text{Co}_3\text{O}_4/\text{NiO}$ composites were manufactured by preparing many molar ratios of Co_3O_4 and NiO, such as 3:1, 2:1, 1:1, 1:2, 1:3, 1:4, and 1:5. Reduced graphene oxide (rGO) is a two-dimensional material with a large specific surface area, excellent carrier mobility, and strong chemical stability. As a function, $\text{Co}_3\text{O}_4/\text{NiO}$ composites were attached to the surface of the rGO sheet. The samples were calcined at various temperatures, including 400 °C, 450 °C, 500 °C, and 550 °C. At a calcined temperature of 400 °C, the $\text{Co}_3\text{O}_4/$

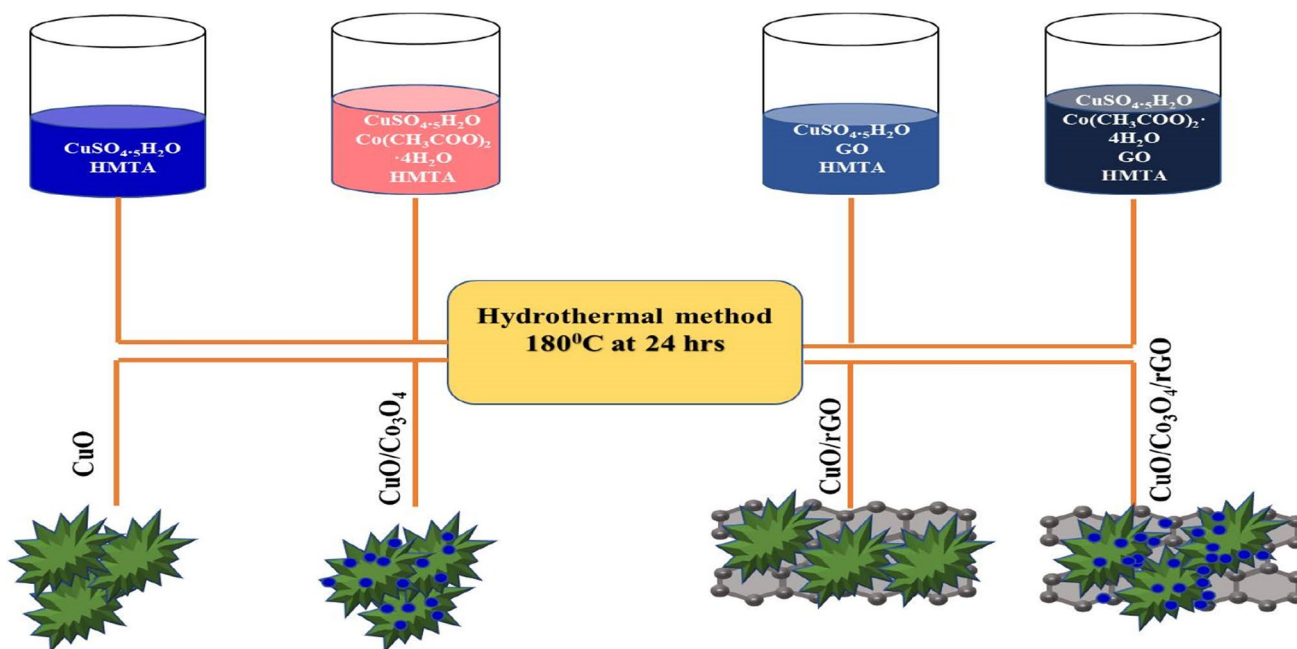
Table 2 Comparison of binary metal oxide/rGO composite material performance

Electrode material	Electrolyte	Specific capacitance	Energy density	Power density	Capacity retention	Ref
NiCo ₂ O ₄ -rGO	2 M KOH	1222 F g ⁻¹ at 0.5 A g ⁻¹	23.32 Wh k g ⁻¹	324.9 W k g ⁻¹	2500 cycles 2.0 A g ⁻¹ is 83%	[103]
Layered NiCo ₂ O ₄ /RGO	6 M KOH	1388 F g ⁻¹ at 0.5 A g ⁻¹	57 Wh k g ⁻¹	375 W k g ⁻¹	90.2% retention after 20,000 cycles at 5 A g ⁻¹	[104]
rGO-NiFe ₂ O ₄	1 M Na ₂ SO ₄	210.9 F g ⁻¹ at 0.5 A g ⁻¹	-	-	No obvious capacity loss even after 5000 cycles	[105]
rGO/MnCo ₂ O ₄	1 M KOH	808 F/g at 2 mV/s	15.2 Wh/kg	7658 W/kg	135% after 1000 charge/discharge cycles	[106]
rGO@NiCo ₂ O ₄	6 M KOH	1040 F/g at 1 A/g	-	-	5000, capacity is decreased to only 12% of its initial value	[107]
NiMoO ₄ /rGO	2 M KOH	1202 F g ⁻¹ at 1 A g ⁻¹	-	-	decrease of 4% after the rest 2000 cycles	[108]
NiMoO ₄ @rGO	2 M KOH	1877 F g ⁻¹ at 1 A g ⁻¹	40 Wh k g ⁻¹	218.2 W g ⁻¹	98% capacitance retention after 4000 cycles at 5 A g ⁻¹	[114]
NiCo ₂ O ₄ -rGO	2 M KOH	777.1 F g ⁻¹ at 5 A g ⁻¹	-	-	99.3% of the capacitance retained after 3000 cycles	[109]
NiCo ₂ O ₄ @RGO	2 M KOH	737 F g ⁻¹ at 1 A g ⁻¹	-	-	6% loss after 3000 charge/discharge cycles at 4 A g ⁻¹	[110]
NiCo ₂ O ₄ /RGO	3 M KOH	947.4 F g ⁻¹ at 0.5 A g ⁻¹	-	-	2.1% after 3000 cycles at the current density of 10 A g ⁻¹	[111]
CoFe ₂ O ₄ /rGO	2 M KOH	551 F/g at 2 mV/s	-	-	98% capacitance retention after 2000 cycles	[112]
rGO/NCO	2 M KOH	613 (1 A g ⁻¹)	9.59 Wh kg ⁻¹	349.46 W kg ⁻¹	90.9%, 2000 cycles	[113]

NiO/rGO composite with a 1:3 ratio had the best performance in supercapacitor electrode material. The Co₃O₄/NiO/rGO composites with 20 mg GO have the significant value CV areas of all the samples, delivering the highest specific capacitance. The Co₃O₄/NiO/rGO system at a current density of 0.5 A/g, a specific capacitance of 325 F/g was attained, with good rate capability. The higher conductivity and efficient exploitation of the surface area of electroactive material in the presence of rGO are attributed to the increased specific capacitance of ternary Co₃O₄/NiO/rGO composites [69]. Prabhu et al. introduced a new supercapacitor electrode material made from 3-dimensional flower-like CuO/Co₃O₄/r-GO hybrid nanocomposites, which were made using a hydrothermal process. Among the four kinds of samples generated by the hydrothermal process are those illustrated in Scheme 8, which include CuO, CuO/Co₃O₄, CuO/rGO, and CuO/Co₃O₄/r-GO. For this research, three-electrode cyclic voltammetry has been used to examine the effect of composite material use on cyclic voltammetry. Because of its excellent electrochemical performance, the CuO/Co₃O₄/r-GO electrode material is regarded as a very promising electrode for high-performance SC applications. The CuO/Co₃O₄/r-GO hybrid composite has a higher surface area than the CuO/Co₃O₄ material because rGO has a larger surface area than the composite material. At a current density of 0.5 Ag⁻¹, the CuO/Co₃O₄/r-GO hybrid composite exhibits a high specific capacitance of 1458 Fg⁻¹, as well as a great rate capacitance and exceptional cyclic stability

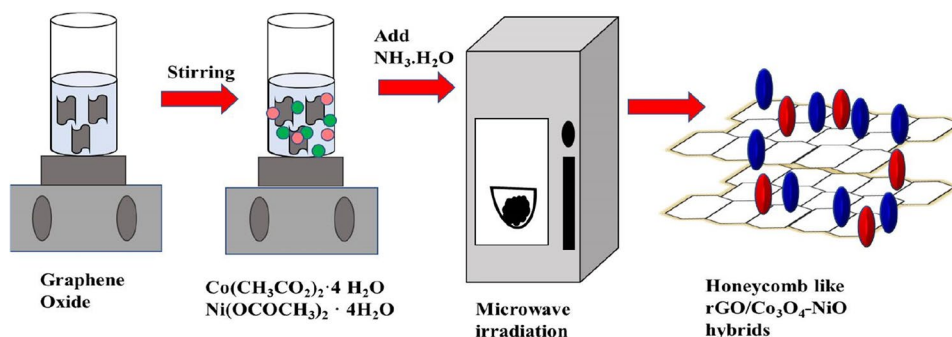
of 97% after 10,000 charging/discharging cycles. The CuO/Co₃O₄/r-GO hybrid composite has a 34.20-Wh kg⁻¹ energy density and a 10,510.30-Wh kg⁻¹ power density. CuO/Co₃O₄/r-GO/NF were also employed as negative and positive electrodes in the solid-state asymmetric supercapacitor device [70].

Wang et al. investigated and optimized flammulina-velutipes-like CeO₂/Co₃O₄/rGO nanoparticles for supercapacitor applications. A high number of flammulina-velutipes are produced in clusters of CeO₂/Co₃O₄/rGO nanoparticles. The purpose of this cluster construction was to increase the surface area of the supercapacitor as well as the material stability of the device. Using a working electrode and a 6 M potassium hydroxide electrolyte solution, the nanoparticles were electrochemically examined. Finally, the electrode material achieved a high specific capacitance of 1606.6 F g⁻¹ at a current density of 1 A g⁻¹, another process in the asymmetric supercapacitor device's performance testing method. When the voltage window was 1.6 V, the power density and energy density (8000 W kg⁻¹ and 47.6 Wh kg⁻¹) were good. After 100,000 continuous charge and discharge cycles, the capacitance retention rate is still extraordinarily high at 96.4% under the condition of 10-Ag⁻¹ current density [71]. R. Kumar et al. synthesized the rGO/Co₃O₄/NiO hybrid nanocomposite by microwave irradiation method shown in Scheme 9. In the first instance, the graphene oxide is produced using a modified Staudenmaier's technique. The rGO/Co₃O₄/NiO hybrid nanocomposite was also used as a



Scheme 8 Synthesis of four different types of electrode material [70]

Scheme 9 Synthesis process of rGO/Co₃O₄/NiO hybrid nano-composite [72]



working electrode in two- and three-electrode configuration systems with 0.1-M KOH electrolytes in this method. The prepared sample is loaded with a glassy carbon electrode (GCE), and the scan rate is changed. The specific capacitance was 910 F g^{-1} , and the cycle performance was excellent, with 89.9% capacitance retention after 2000 cycles. This seems to be owing to the belief that the honeycomb-like open edges of the rGO are fully covered by Co₃O₄/NiO composite material in this morphological structure, allowing the hybrid material to achieve the greatest specific capacitance and cyclic stability while operating at a low scan rate [72].

G. S. Kumar et al. designed a composite electrode material composed of CeO₂-SnO₂/rGO for supercapacitor applications. This composite was developed using a low-temperature hydrothermal method. The modified Hummer's technique was also used to prepare graphene oxide. In this supercapacitor application, six different kinds of electrodes are produced using a hydrothermal method, including CeO₂,

SnO₂, and CeO₂-SnO₂ with 0.08–0.02 M, 0.05–0.05 M, and CeO₂-SnO₂/rGO, as appropriate, in order to achieve the desired performance. The rGO sheet completely encapsulated the spherical CeO₂-SnO₂ nanoparticle in its entirety. When compared to the other electrode materials, the performance of the ternary CeO₂-SnO₂/rGO composite established a specific capacitance of 156 Fg^{-1} at a current density of 0.5 A g^{-1} [73]. M. Geerthana et al. found that using a simple on-site hydrothermal technique, they could synthesize $\alpha\text{-Fe}_2\text{O}_3$ nanoparticles, binary $\alpha\text{-Fe}_2\text{O}_3/\text{rGO}$, and ternary $\alpha\text{-Fe}_2\text{O}_3/\text{SnO}_2/\text{rGO}$ nanocomposites. Their electrode technology makes use of the synthesized materials as electrode materials for supercapacitor applications. In comparison to nanoparticles of $\alpha\text{-Fe}_2\text{O}_3$, a ternary $\alpha\text{-Fe}_2\text{O}_3/\text{SnO}_2/\text{rGO}$ nanocomposite exhibited 821 Fg^{-1} of specific capacitance at a current density of 1 Ag^{-1} . The ternary composite has retained over 98% of the initial cycle capacity after 10,000 cycles at 10 A g^{-1} . It was the individual components in the

Table 3 Comparison of three electrode and device

Material	Three-electrode specific capacitance	Two-electrode specific capacitance	Ref
Co ₃ O ₄ -rGO	1328 Cg ⁻¹ at 2 A g ⁻¹	80 F g ⁻¹ at 0.1 A g ⁻¹	[44]
NiCo ₂ O ₄ /rGO	702 F g ⁻¹ at 0.5 A g ⁻¹	259 F g ⁻¹ at 0.5 A g ⁻¹	[56]
NiMoO ₄ -rGO	1274 Fg ⁻¹ at 1 A g ⁻¹	295 F g ⁻¹ at 1 A g ⁻¹	[58]
ZnCo ₂ O ₄ -rGO	3222 F g ⁻¹ at 1 A g ⁻¹	139 F g ⁻¹ at 0.5 A g ⁻¹	[66]
CuO/Co ₃ O ₄ /r-GO	1458 Fg ⁻¹ at 0.5 A g ⁻¹	198 F g ⁻¹ at 2 A g ⁻¹	[70]
CeO ₂ /Co ₃ O ₄ /rGO	1606.6 F g ⁻¹ at 1 A g ⁻¹	192.2 F g ⁻¹ at 1 A g ⁻¹	[71]
α-Fe ₂ O ₃ /SnO ₂ /rGO	821 Fg ⁻¹ at 1 A g ⁻¹	92.6 F g ⁻¹ at 1 A g ⁻¹	[74]

ternary α-Fe₂O₃/SnO₂/rGO nanocomposite that each contributed to the specific capacitance being improved. Reduced graphene oxide has helped in the development of the electrical conductivity and surface area of the nanocomposite by increasing its surface area. The asymmetric supercapacitor gives amazing specific capacitance, energy, and power densities in the 0.0–1.4-V potential range in alkaline polymer electrolyte and 92.59% capacitance retention after 5000 cycles (Table 3) [74].

4 Conclusion

In summary, different preparation techniques for reduced graphene oxide (rGO)/transition metal oxide composite electrodes have been examined. These composites have extraordinary supercapacitive capability. Because of their large surface area, high conductivity, and manufacturability, synergistic evaluations of a composite material have a significant effect on the enhanced supercapacitive properties of the synthesized materials. Reduced graphene oxide has been used to create composites with transition metal oxide; it provides mechanical support for the transition metal oxide structure, significantly improving cycle performance as well as specific capacitance. The performance of supercapacitor was also affected by synthesis methods and different electrolytes. In this context, rGO-based metal oxide is the best way to synthesis composite electrode with metal oxides or conducting polymers. It has been noticed that rGO plays an important role for enhancing the overall properties like capacitance, power density, energy density, and cyclic retention. The above results suggest that rGO/metal oxide composite materials are mainly used for energy storage applications.

Funding R. Kumar was provided financial support by Periyar University in the form of University Research Fellowship.

Declarations

Conflict of interest The authors declare no competing interests.

References

1. Harish Kumar, Rahul Sharma, Ankita Yadav, Rajni Kumari, Recent advancement made in the field of reduced graphene oxide-based nanocomposites used in the energy storage devices: a review, *J. Energy Storage*. **33**, 102032 (2021). <https://doi.org/10.1016/j.est.2020.102032>
2. D.T. Phat, P.M. Thao, N. Van Nghia, L.T. Son, T.V. Thu, N.T. Lan, N.Q. Quyen, N. Van Ky, T. Van Nguyen, Morphology controlled synthesis of battery-type NiCo₂O₄ supported on nickel foam for high performance hybrid supercapacitors, *J. Energy Storage*. **33**, 102030 (2021). <https://doi.org/10.1016/j.est.2020.102030>
3. K. Mohamed Racik, A. Manikandan, M. Mahendiran, P. Prabhakaran, J. Madhavan, M. Victor Antony Raj, Fabrication of manganese oxide decorated copper oxide (MnO₂/CuO) nanocomposite electrodes for energy storage supercapacitor devices, *Phys. E Low-Dimensional Syst. Nanostructures*. **119**, 114033 (2020). <https://doi.org/10.1016/j.physe.2020.114033>
4. C.I. Priyadharsini, G. Marimuthu, T. Pazhanivel, P.M. Anbarasan, V. Aroulmoji, V. Siva, L. Mohana, Sol-gel synthesis of Co₃O₄ nanoparticles as an electrode material for supercapacitor applications. *J. Sol-Gel Sci. Technol.* **96**, 416–422 (2020). <https://doi.org/10.1007/s10971-020-05393-x>
5. G. Luo, H. Li, D. Zhang, L. Gao, T. Lin, A template-free synthesis via alkaline route for Nb₂O₅/carbon nanotubes composite as pseudo-capacitor material with high-rate performance. *Electrochim. Acta*. **235**, 175–181 (2017). <https://doi.org/10.1016/j.electacta.2017.03.112>
6. W.G. Nunes, R. Vicentini, B.G.A. Freitas, F.E.R. Oliveira, A.M.P. Marque, R.M. Filho, G. Doubek, L.M. Da Silva, H. Zanin, Pseudo-capacitive behavior of multi-walled carbon nanotubes decorated with nickel and manganese (hydr)oxides nanoparticles. *J. Energy Storage*. **31**, 101583 (2020). <https://doi.org/10.1016/j.est.2020.101583>
7. D. Xuan, W. Chengyang, C. Mingming, J. Yang, W. Jin, Electrochemical performances of nanoparticle Fe₃O₄/activated carbon supercapacitor using KOH electrolyte solution. *J. Phys. Chem. C*. **113**, 2643–2646 (2009). <https://doi.org/10.1021/jp8088269>
8. G. Milczarek, A. Ciszewski, I. Stepniak, Oxygen-doped activated carbon fiber cloth as electrode material for electrochemical capacitor. *J. Power Sources*. **196**, 7882–7885 (2011). <https://doi.org/10.1016/j.jpowsour.2011.04.046>
9. W.H. Low, S.S. Lim, C.W. Siong, C.H. Chia, P.S. Khiew, One dimensional MnV₂O₆ nanobelts on graphene as outstanding electrode material for high energy density symmetric supercapacitor. *Ceram. Int.* **47**, 9560–9568 (2021). <https://doi.org/10.1016/j.ceramint.2020.12.090>
10. S.A. Delbari, L.S. Ghadimi, R. Hadi, S. Farhoudian, M. Nedaei, A. Babapoor, A. Sabahi Namini, Q. Van Le, M. Shokouhimehr, M. Shahedi Asl, M. Mohammadi, Transition metal oxide-based electrode materials for flexible supercapacitors: a review, *J. Alloys Compd.* **857**, 158281 (2021). <https://doi.org/10.1016/j.jallcom.2020.158281>

11. P. Wang, Y.J. Zhao, L.X. Wen, J.F. Chen, Z.G. Lei, Ultrasound-microwave-assisted synthesis of MnO₂ supercapacitor electrode materials. *Ind. Eng. Chem. Res.* **53**, 20116–20123 (2014). <https://doi.org/10.1021/ie5025485>
12. Y.Q. Zhang, L. Li, S.J. Shi, Q.Q. Xiong, X.Y. Zhao, X.L. Wang, C.D. Gu, J.P. Tu, Synthesis of porous Co₃O₄ nanoflake array and its temperature behavior as pseudo-capacitor electrode. *J. Power Sources.* **256**, 200–205 (2014). <https://doi.org/10.1016/j.jpowsour.2014.01.073>
13. H.Z. Yang, J.P. Zou, Controllable preparation of hierarchical NiO hollow microspheres with high pseudo-capacitance. *Trans Nonferrous Met Soc China English Ed.* **28**, 1808–1818 (2018). [https://doi.org/10.1016/S1003-6326\(18\)64825-3](https://doi.org/10.1016/S1003-6326(18)64825-3)
14. J. Huang, S. Yang, Y. Xu, X. Zhou, X. Jiang, N. Shi, D. Cao, J. Yin, G. Wang, Fe₂O₃ sheets grown on nickel foam as electrode material for electrochemical capacitors. *J. Electroanal. Chem.* **713**, 98–102 (2014). <https://doi.org/10.1016/j.jelechem.2013.12.009>
15. J. Rajeswari, P.S. Kishore, B. Viswanathan, T.K. Varadarajan, One-dimensional MoO₂ nanorods for supercapacitor applications. *Electrochem. Commun.* **11**, 572–575 (2009). <https://doi.org/10.1016/j.elecom.2008.12.050>
16. J. Zhang, J. Ma, L.L. Zhang, P. Guo, J. Jiang, X.S. Zhao, Template synthesis of tubular ruthenium oxides for supercapacitor applications. *J Phys Chem C* **114**(13), 608–13,613 (2010). <https://doi.org/10.1021/jp105146c>
17. M. Li, G. Sun, P. Yin, C. Ruan, K. Ai, Controlling the formation of rodlike V₂O₅ nanocrystals on reduced graphene oxide for high-performance supercapacitors. *ACS Appl. Mater. Interfaces.* **5**, 11462–11470 (2013). <https://doi.org/10.1021/am403739g>
18. S. Suthakaran, S. Dhanapandian, N. Krishnakumar, N. Ponpandian, P. Dhamodharan, M. Anandan, Surfactant-assisted hydrothermal synthesis of Zr doped SnO₂ nanoparticles with photocatalytic and supercapacitor applications, *Mater. Sci. Semicond. Process.* **111**, 104982 (2020). <https://doi.org/10.1016/j.mssp.2020.104982>
19. A. Ramadoss, S.J. Kim, Improved activity of a graphene-TiO₂ hybrid electrode in an electrochemical supercapacitor. *Carbon N Y* **63**, 434–445 (2013). <https://doi.org/10.1016/j.carbon.2013.07.006>
20. Y. Zhang, L. Cheng, L. Zhang, D. Yang, C. Du, L. Wan, J. Chen, M. Xie, Effect of conjugation level on the performance of porphyrin polymer based supercapacitors, *J. Energy Storage.* **34**, 102018 (2021). <https://doi.org/10.1016/j.est.2020.102018>
21. S. Khamlich, Z. Abdullaev, J.V. Kennedy, M. Maaza, High performance symmetric supercapacitor based on zinc hydroxy-chloride nanosheets and 3D graphene-nickel foam composite. *J. Electrochimica Acta* **303**, 246–256 (2019). <https://doi.org/10.1016/j.apsusc.2017.02.095>
22. B.K. Saikia, S.M. Benoy, M. Bora, J. Tamuly, M. Pandey, D. Bhattacharya, A brief review on supercapacitor energy storage devices and utilization of natural carbon resources as their electrode materials, *Fuel.* **282**, 118796 (2020). <https://doi.org/10.1016/j.fuel.2020.118796>
23. S. Korkmaz, A. Kariper, Graphene and graphene oxide based aerogels: synthesis, characteristics and supercapacitor applications. *J. Energy Storage.* **27**, 101038 (2020). <https://doi.org/10.1016/j.est.2019.101038>
24. B. Xu, S. Yue, Z. Sui, X. Zhang, S. Hou, G. Cao, Y. Yang, What is the choice for supercapacitors: graphene or graphene oxide? *Energy Environ. Sci.* **4**, 2826–2830 (2011). <https://doi.org/10.1039/c1ee01198g>
25. H. Wang, Q. Fu, C. Pan, Green mass synthesis of graphene oxide and its MnO₂ composite for high performance supercapacitor. *Electrochim Acta* **312**, 11–21 (2019). <https://doi.org/10.1016/j.electacta.2019.04.178>
26. J. Jayachandiran, J. Yesuraj, M. Arivanandhan, A. Raja, S.A. Suthanthiraraj, R. Jayavel, D. Nedumaran, Synthesis and electrochemical studies of rGO/ZnO nanocomposite for supercapacitor application. *J Inorg Organomet Polym Mater* **28**, 2046–2055 (2018). <https://doi.org/10.1007/s10904-018-0873-0>
27. R. Kumar, E. Joanni, R.K. Singh, D.P. Singh, S.A. Moshkalev, Recent advances in the synthesis and modification of carbon-based 2D materials for application in energy conversion and storage. *J. Progress in Energy and Combustion Science* **67**, 115–157 (2018). <https://doi.org/10.1016/j.peccs.2018.03.001>
28. R. Kumar, S. Sahoo, E. Joanni, R.K. Singh, K. Maegawa, W.K. Tan, G.K. Kamal, K. Kar, A. Matsuda, Heteroatom doped graphene engineering for energy storage and conversion. *Mater Today* **39**, 47–65 (2020). <https://doi.org/10.1016/j.mattod.2020.04.010>
29. R. Kumar, R.K. Singh, P.K. Dubey, P. Kumar, R.S. Tiwari, I.K. Oh, Pressure-dependent synthesis of high-quality few-layer graphene by plasma-enhanced arc discharge and their thermal stability. *J Nanopart Res* **15**, 1847 (2013). <https://doi.org/10.1007/s11051-013-1847-3>
30. Rajesh Kumar, Sumanta Sahoo, Ednan Joanni, Rajesh Kumar Singh, Ram Manohar Yadav, Rajiv Kumar, Verma, Dinesh Pratap Singh, Wai Kian Tan, Angel Pérez del Pino, Stanislav A. Moshkalev, and Atsunori Matsuda, A review on synthesis of graphene, h-BN and MoS₂ for energy storage, applications: recent progress and perspectives, *J. Nano Research* **12**(11), 2655–2694, 2019. <https://doi.org/10.1007/s12274-019-2467-8>
31. R. Kumar, R.K. Singh, D.P. Singh, E. Joanni, R.M. Yadav, S.A. Moshkalev, Laser-assisted synthesis, reduction and micro-patterning of graphene recent progress and applications. *J Coordination Chemistry Rev* **342**, 34–79 (2017). <https://doi.org/10.1016/j.ccr.2017.03.021>
32. Rajesh Kumar, Sumanta Sahoo, Ednan Joanni, Rajesh K. Singh, Kamal K. Kar, Microwave as a tool for synthesis of carbon-based electrodes for energy storage, *ACS Applied Materials & Interfaces* (2021). <https://doi.org/10.1021/acscami.1c15934>
33. N. Devi, S. Sahoo, R. Kumar, R.K. Singh, A review of the microwave-assisted synthesis of carbon nanomaterials metal oxides/hydroxides and their composites for energy storage applications. *J Nanoscale* **13**, 11679–11711 (2021). <https://doi.org/10.1039/D1NR01134K>
34. R. Kumar, S. Sahoo, E. Joanni, R.K. Singh, W.K. Tan, K.K. Kar, A. Matsuda, Recent progress in the synthesis of graphene and derived materials for next generation electrodes of high performance lithium ion batteries. *J Prog in Energy and Combust Sci* **75**, 100786 (2019). <https://doi.org/10.1016/j.peccs.2019.100786>
35. N. Cao, Y. Zhang, Study of Reduced graphene oxide preparation by Hummers' method and related characterization, *J. Nanomater.* **2015**, 168125 (2015). <https://doi.org/10.1155/2015/168125>
36. S.N. Alam, N. Sharma, L. Kumar, Synthesis of graphene oxide (GO) by modified Hummers method and its thermal reduction to obtain reduced graphene oxide (rGO). *Graphene* **06**, 1–18 (2017). <https://doi.org/10.4236/graphene.2017.61001>
37. R. Thangappan, S. Kalaiselvam, A. Elayaperumal, R. Jayavel, M. Arivanandhan, R. Karthikeyan, Y. Hayakawa, Graphene decorated with MoS₂ nanosheets: a synergetic energy storage composite electrode for supercapacitor applications. *Dalton Trans.* **45**, 2637–2646 (2016). <https://doi.org/10.1039/C5DT04832J>
38. A. Alkhouzaam, H. Qiblawey, M. Khraisheh, M. Atieh, M. Al-Ghouti, Synthesis of graphene oxides particle of high oxidation degree using a modified Hummers method. *Ceram Int* **46**, 23997–24007 (2020). <https://doi.org/10.1016/j.ceramint.2020.06.177>
39. L. Sun, B. Fugetsu, Mass production of graphene oxide from expanded graphite. *Mater. Lett.* **109**, 207–210 (2013). <https://doi.org/10.1016/j.matlet.2013.07.072>

40. P. Kumar, S. Penta, S.P. Mahapatra, Dielectric properties of graphene oxide synthesized by modified Hummers' method from graphite powder. *Integr Ferroelectr* **202**, 41–51 (2019). <https://doi.org/10.1080/10584587.2019.1674822>
41. M. Sohail, M. Saleem, S. Ullah, N. Saeed, A. Afridi, M. Khan, M. Arif, Modified and improved Hummer's synthesis of graphene oxide for capacitors applications. *Mod Electron Mater* **3**, 110–116 (2017). <https://doi.org/10.1016/j.moem.2017.07.002>
42. J. Xu, L. Wu, Y. Liu, J. Zhang, J. Liu, S. Shu, X. Kang, Q. Song, D. Liu, F. Huang, Y. Hu, NiO-rGO composite for supercapacitor electrode, *Surfaces and Interfaces*. **18**, 100420 (2020). <https://doi.org/10.1016/j.surfin.2019.100420>
43. Y. Zhu, S. Cheng, W. Zhou, J. Jia, L. Yang, M. Yao, M. Wang, J. Zhou, P. Wu, M. Liu, Construction and performance characterization of α -Fe₂O₃/rGO composite for long-cycling-life supercapacitor anode. *ACS Sustain Chem Eng* **5**, 5067–5074 (2017). <https://doi.org/10.1021/acssuschemeng.7b00445>
44. S. Raj, S.K. Srivastava, P. Kar, P. Roy, In situ growth of Co₃O₄ nanoflakes on reduced graphene oxide-wrapped Ni-foam as high performance asymmetric supercapacitor. *Electrochim Acta* **302**, 327–337 (2019). <https://doi.org/10.1016/j.electacta.2019.02.010>
45. N.A. Devi, S. Nongthombam, S. Sinha, R. Bhujel, S. Rai, W.I. Singh, P. Dasgupta, B.P. Swain, Investigation of chemical bonding and supercapacitivity properties of Fe₃O₄-rGO nanocomposites for supercapacitor applications, *Diam. Relat. Mater.* **104**, 107756 (2020). <https://doi.org/10.1016/j.diamond.2020.107756>
46. S. Ghasemi, S.R. Hosseini, O. Boore-talari, Sonochemical assisted synthesis MnO₂/RGO nanohybrid as effective electrode material for supercapacitor. *Ultrason Sonochem* **40**, 675–685 (2018). <https://doi.org/10.1016/j.ultsonch.2017.08.013>
47. Y.N. Sudhakar, H. Hemant, S.S. Nitinkumar, P. Poornesh, M. Selvakumar, Green synthesis and electrochemical characterization of rGO–CuO nanocomposites for supercapacitor applications. *Ionics (Kiel)* **23**, 1267–1276 (2017). <https://doi.org/10.1007/s11581-016-1923-7>
48. Y. Zhang, M. Liu, S. Sun, L. Yang, The preparation and characterization of SnO₂/rGO nanocomposites electrode materials for supercapacitor, *Adv. Compos. Lett.* **29**, 1–7 (2020). <https://doi.org/10.1177/2633366X20909839>
49. F. Du, X. Zuo, Q. Yang, G. Li, Z. Ding, M. Wu, Y. Ma, S. Jin, K. Zhu, Facile hydrothermal reduction synthesis of porous Co₃O₄ nanosheets@RGO nanocomposite and applied as a supercapacitor electrode with enhanced specific capacitance and excellent cycle stability. *Electrochim Acta* **222**, 976–982 (2016). <https://doi.org/10.1016/j.electacta.2016.11.065>
50. C. Lai, Y. Sun, B. Lin, Synthesis of sandwich-like porous nanostructure of Co₃O₄-rGO for flexible all-solid-state high-performance asymmetric supercapacitors, *Mater. Today. Energy* **13**, 342–352 (2019). <https://doi.org/10.1016/j.mtener.2019.06.008>
51. Y. Chen, X. Zhang, D. Zhang, Y. Ma, One-pot hydrothermal synthesis of ruthenium oxide nanodots on reduced graphene oxide sheets for supercapacitors. *J Alloys Compd* **511**, 251–256 (2012). <https://doi.org/10.1016/j.jallcom.2011.09.045>
52. A. Viswanathan, A.N. Shetty, Reduced graphene oxide/vanadium pentoxide nanocomposite as electrode material for highly rate capable and durable supercapacitors, *J. Energy Storage*. **27**, 101103 (2020). <https://doi.org/10.1016/j.est.2019.101103>
53. Z. Wu, Y. Zhu, X. Ji, C.E. Banks, Transition metal oxides as supercapacitor materials. *Nanomaterials in Advanced Batteries and Supercapacitors* 317–344 (2016). https://doi.org/10.1007/978-3-319-26082-2_9
54. A.N. Naveen, S. Selladurai, Novel low temperature synthesis and electrochemical characterization of mesoporous nickel cobaltite-reduced graphene oxide (RGO) composite for supercapacitor application. *Electrochim Acta* **173**, 290–301 (2015). <https://doi.org/10.1016/j.electacta.2015.05.072>
55. M.B. Askari, P. Salarizadeh, Binary nickel ferrite oxide (NiFe₂O₄) nanoparticles coated on reduced graphene oxide as stable and high-performance asymmetric supercapacitor electrode material. *Int J Hydrogen Energy* **45**, 27482–27491 (2020). <https://doi.org/10.1016/j.ijhydene.2020.07.063>
56. F. Meng, L. Zhao, Y. Zhang, J. Zhai, Y. Li, W. Zhang, Facile synthesis of NiCo₂O₄/rGO microspheres with high-performance for supercapacitor. *Ceram Int* **45**, 23701–23706 (2019). <https://doi.org/10.1016/j.ceramint.2019.08.085>
57. Z. Wang, Z. Zhu, C. Zhang, C. Xu, C. Chen, Facile synthesis of reduced graphene oxide/NiMn₂O₄ nanorods hybrid materials for high-performance supercapacitors. *Electrochim Acta* **230**, 438–444 (2017). <https://doi.org/10.1016/j.electacta.2017.02.023>
58. T. Liu, H. Chai, D. Jia, Y. Su, T. Wang, W. Zhou, Rapid microwave-assisted synthesis of mesoporous NiMoO₄ nanorod/reduced graphene oxide composites for high-performance supercapacitors. *Electrochim Acta* **180**, 998–1006 (2015). <https://doi.org/10.1016/j.electacta.2015.07.175>
59. X. Xu, J. Shen, N. Li, M. Ye, Microwave-assisted synthesis of graphene/CoMoO₄ nanocomposites with enhanced supercapacitor performance. *J. Alloys Compd* **616**, 58–65 (2014). <https://doi.org/10.1016/j.jallcom.2014.07.047>
60. Y. Yuan, H. Bi, G. He, J. Zhu, H. Chen, A facile hydrothermal synthesis of a MnCo₂O₄@reduced graphene oxide nanocomposite for application in supercapacitors. *Chem Lett* **43**, 83–85 (2014). <https://doi.org/10.1246/cl.130815>
61. P. He, K. Yang, W. Wang, F. Dong, L. Du, Y. Deng, Reduced graphene oxide-CoFe₂O₄ composites for supercapacitor electrode. *Russ J Electrochem* **49**, 359–364 (2013). <https://doi.org/10.1134/S1023193513040101>
62. A.J.C. Mary, A.C. Bose, Facile synthesis of ZnCo₂O₄/rGO nanocomposite for effective supercapacitor application. *AIP Conf. Proc.* **1832**, 050093 (2017). <https://doi.org/10.1063/1.4980326>
63. M. Isacfranklin, G. Ravi, R. Yuvakkumar, P. Kumar, D. Velauthapillai, B. Saravanakumar, M. Thambidurai, C. Dang, Urchin like NiCo₂O₄/rGO nanocomposite for high energy asymmetric storage applications. *Ceram Int* **46**, 16291–16297 (2020). <https://doi.org/10.1016/j.ceramint.2020.03.186>
64. Y.Z. Cai, W.Q. Cao, P. He, Y.L. Zhang, M.S. Cao, NiFe₂O₄ nanoparticles on reduced graphene oxide for supercapacitor electrodes with improved capacitance, *Mater. Res. Express*. **6**, 105535 (2019). <https://doi.org/10.1088/2053-1591/ab3fff>
65. C. Zhang, X. Geng, S. Tang, M. Deng, Y. Du, NiCo₂O₄@rGO hybrid nanostructures on Ni foam as high-performance supercapacitor electrodes. *J Mater Chem A* **5**, 5912–5919 (2017). <https://doi.org/10.1039/c7ta00571g>
66. Z. Gao, L. Zhang, J. Chang, Z. Wang, D. Wu, F. Xu, Y. Guo, K. Jiang, ZnCo₂O₄-reduced graphene oxide composite with balanced capacitive performance in asymmetric supercapacitors. *Appl Surf Sci* **442**, 138–147 (2018). <https://doi.org/10.1016/j.apsusc.2018.02.152>
67. Y. Mao, T.J. Park, S.S. Wong, Synthesis of classes of ternary metal oxide nanostructures, *Chem. Commun.* **46**, 5721–5735 (2005). <https://doi.org/10.1039/b509960a>
68. D. Chen, Q. Wang, R. Wang, G. Shen, Ternary oxide nanostructured materials for supercapacitors: a review. *J Mater Chem A* **3**, 10158–10173 (2015). <https://doi.org/10.1039/c4ta06923d>
69. J. Wu, Q. Zhou, L. Lin, Q. Luo, Lu, Ternary Co₃O₄/NiO/reduced graphene oxide hybrid composites with improved electrochemical properties. *Ceram Int* **45**, 15394–15399 (2019). <https://doi.org/10.1016/j.ceramint.2019.05.035>
70. S. Prabhu, S. Sohila, D. Navaneethan, S. Harish, M. Navaneethan, R. Ramesh, Three dimensional flower-like CuO/Co₃O₄/r-GO

- heterostructure for high-performance asymmetric supercapacitors, *J. Alloys Compd.* **846**, 156439 (2020). <https://doi.org/10.1016/j.jallcom.2020.156439>
71. Z. Wang, K. Zhao, S. Lu, W. Xu, Application of flammulina-velutipes-like $\text{CeO}_2/\text{Co}_3\text{O}_4/\text{rGO}$ in high-performance asymmetric supercapacitors, *Electrochim. Acta.* **353**, 136599 (2020). <https://doi.org/10.1016/j.electacta.2020.136599>
 72. R. Kumar, S.M. Youssry, H.M. Soe, M.M. Abdel-Galeil, G. Kawamura, A. Matsuda, Honeycomb-like open-edged reduced-graphene-oxide-enclosed transition metal oxides ($\text{NiO}/\text{Co}_3\text{O}_4$) as improved electrode materials for high-performance supercapacitor, *J. Energy Storage.* **30**, 101539 (2020). <https://doi.org/10.1016/j.est.2020.101539>
 73. G.S. Kumar, S.A. Reddy, H. Maseed, N.R. Reddy, Facile hydrothermal synthesis of ternary $\text{CeO}_2\text{-SnO}_2/\text{rGO}$ nanocomposite for supercapacitor application, *Funct. Mater. Lett.* **13**, 2051005 (2020). <https://doi.org/10.1142/S1793604720510054>
 74. M. Geerthana, S. Prabhu, S. Harish, M. Navaneethan, R. Ramesh, M. Selvaraj, Design and preparation of ternary $\alpha\text{-Fe}_2\text{O}_3/\text{SnO}_2/\text{rGO}$ nanocomposite as an electrode material for supercapacitor, *J. Mater. Sci. Mater. Electron.* (2021). <https://doi.org/10.1007/s10854-021-06128-6>
 75. K.K. Purushothaman, B. Saravanakumar, I.M. Babu, B. Sethuraman, G. Muralidharan, Nanostructured $\text{CuO}/\text{reduced graphene oxide}$ composite for hybrid supercapacitors, *RSC Adv* **4**, 23485–23491 (2014). <https://doi.org/10.1039/c4ra02107j>
 76. V.M. Vimuna, A.R. Athira, K. V. Dinesh Babu, T.S. Xavier, Simultaneous stirring and microwave assisted synthesis of nanoflakes MnO_2/rGO composite electrode material for symmetric supercapacitor with enhanced electrochemical performance, *Diam. Relat. Mater.* **110**, 108129 (2020). <https://doi.org/10.1016/j.diamond.2020.108129>
 77. Y. Zhang, Y. Shen, X. Xie, W. Du, L. Kang, Y. Wang, X. Sun, Z. Li, B. Wang, One-step synthesis of the reduced graphene oxide@ NiO composites for supercapacitor electrodes by electrode-assisted plasma electrolysis, *Mater. Des.* **196**, 109111 (2020). <https://doi.org/10.1016/j.matdes.2020.109111>
 78. Q. Li, Q. Wei, L. Xie, C. Chen, C. Lu, F.Y. Su, P. Zhou, Layered $\text{NiO}/\text{reduced graphene oxide}$ composites by heterogeneous assembly with enhanced performance as high-performance asymmetric supercapacitor cathode, *RSC Adv* **6**, 46,548–46,557 (2016). <https://doi.org/10.1039/c6ra04998b>
 79. D. Zhang, W. Zou, Decorating reduced graphene oxide with Co_3O_4 hollow spheres and their application in supercapacitor materials, *Curr Appl Phys* **13**, 1796–1800 (2013). <https://doi.org/10.1016/j.cap.2013.07.001>
 80. Z. Huang, S. Li, Z. Li, J. Li, G. Zhang, L. Cao, H. Liu, Mn_3O_4 nanoflakes/ rGO composites with moderate pore size and (O=) C-O-Mn bond for enhanced supercapacitor performance, *J. Alloys Compd.* **830**, 154637 (2020). <https://doi.org/10.1016/j.jallcom.2020.154637>
 81. A.K. Das, S. Sahoo, P. Arunachalam, S. Zhang, J.J. Shim, Facile synthesis of Fe_3O_4 nanorod decorated reduced graphene oxide (RGO) for supercapacitor application, *RSC Adv* **6**, 107,057–107,064 (2016). <https://doi.org/10.1039/c6ra23665k>
 82. X. Dong, K. Wang, C. Zhao, X. Qian, S. Chen, Z. Li, H. Liu, S. Dou, Direct synthesis of $\text{RGO}/\text{Cu}_2\text{O}$ composite films on Cu foil for supercapacitors, *J. Alloys Compd.* **586**, 745–753 (2014). <https://doi.org/10.1016/j.jallcom.2013.10.078>
 83. Y. Zhou, X. Zou, Z. Zhao, B. Xiang, Y. Zhang, CoO/rGO composite prepared by a facile direct-flame approach for high-power supercapacitors, *Ceram Int* **44**, 16900–16907 (2018). <https://doi.org/10.1016/j.ceramint.2018.06.128>
 84. S. Sundriyal, M. Sharma, A. Kaur, S. Mishra, A. Deep, Improved electrochemical performance of rGO/TiO_2 nanosheet composite based electrode for supercapacitor applications, *J. Mater. Sci. Mater. Electron* **29**, 12754–12764 (2018). <https://doi.org/10.1007/s10854-018-9393-5>
 85. Y. Hu, C. Guan, Q. Ke, Z.F. Yow, C. Cheng, J. Wang, Hybrid Fe_2O_3 nanoparticle clusters/ rGO paper as an effective negative electrode for flexible supercapacitors, *Chem Mater* **28**, 7296–7303 (2016). <https://doi.org/10.1021/acs.chemmater.6b02585>
 86. I.Y.Y. Bu, R. Huang, Fabrication of CuO -decorated reduced graphene oxide nanosheets for supercapacitor applications, *Ceram Int* **43**, 45–50 (2017). <https://doi.org/10.1016/j.ceramint.2016.08.136>
 87. S. Sundriyal, V. Shrivastav, M. Sharma, S. Mishra, A. Deep, Significantly enhanced performance of rGO/TiO_2 nanosheet composite electrodes based 1.8 V symmetrical supercapacitor with use of redox additive electrolyte, *J. Alloys Compd* **790**, 377–387 (2019). <https://doi.org/10.1016/j.jallcom.2019.03.150>
 88. Y. Zhou, L. Guo, W. Shi, X. Zou, B. Xiang, S. Xing, Rapid production of $\text{Mn}_3\text{O}_4/\text{rGO}$ as an efficient electrode material for supercapacitor by flame plasma, *Materials (Basel)* **11**, 881 (2018). <https://doi.org/10.3390/ma11060881>
 89. L.J. Xie, J.F. Wu, C.M. Chen, C.M. Zhang, L. Wan, J.L. Wang, Q.Q. Kong, C.X. Lv, K.X. Li, G.H. Sun, A novel asymmetric supercapacitor with an activated carbon cathode and a reduced graphene oxide-cobalt oxide nanocomposite anode, *J. Power Sources* **242**, 148–156 (2013). <https://doi.org/10.1016/j.jpowsour.2013.05.081>
 90. C. Xiang, M. Li, M. Zhi, A. Manivannan, N. Wu, Reduced graphene oxide/titanium dioxide composites for supercapacitor electrodes shape and coupling effects, *J. Mater. Chem* **22**, 19161–19167 (2012). <https://doi.org/10.1039/c2jm33177b>
 91. D. Govindarajan, V.U. Shankar, R. Gopalakrishnan, Supercapacitor behavior and characterization of RGO anchored V_2O_5 nanorods, *J. Mater. Sci. Mater. Electron* **30**, 16,142–16,155 (2019). <https://doi.org/10.1007/s10854-019-01984-9>
 92. C.Y. Foo, A. Sumboja, D.J.H. Tan, J. Wang, P.S. Lee, Flexible and highly scalable $\text{V}_2\text{O}_5\text{-rGO}$ electrodes in an organic electrolyte for supercapacitor devices, *Adv. Energy Mater.* **4**, 1400236 (2014). <https://doi.org/10.1002/aenm.201400236>
 93. I.S. El-Hallag, M.N. El-Nahass, S.M. Youssry, R. Kumar, M.M. Abdel-Galeil, A. Matsud, Facile in-situ simultaneous electrochemical reduction and deposition of reduced graphene oxide embedded palladium nanoparticles as high performance electrode materials for supercapacitor with excellent rate capability, *J. Electrochimica Acta* **314**, 124–134 (2019). <https://doi.org/10.1016/j.electacta.2019.05.065>
 94. R. Kumar, S. Sahoo, W.K. Tan, G. Kawamura, A. Matsud, K.K. Kar, Microwave-assisted thin reduced graphene oxide-cobalt oxide nanoparticles as hybrids for electrode materials in supercapacitor, *J. of Energy Storage* **40**, 102724 (2021). <https://doi.org/10.1016/j.est.2021.102724>
 95. R. Kumar, S.M. Youssry, M.M. Abdel-Galeil, A. Matsuda, One-pot synthesis of reduced graphene oxide nanosheets anchored ZnO nanoparticles via microwave approach for electrochemical performance as supercapacitor electrode, *J. Mater. Sci. Mater. Electron* **31**, 15456–15465 (2020). <https://doi.org/10.1007/s10854-020-04108-w>
 96. S.M. Youssry, M.N. El-Nahass, R. Kumar, I.S. El-Hallag, W.K. Tan, A. Matsuda, Superior performance of $\text{Ni}(\text{OH})_2\text{-ErGO}@\text{NF}$ electrode materials as pseudocapacitance using electrochemical deposition via two simple successive steps, *J. of Energy Storage* **30**, 101485 (2020). <https://doi.org/10.1016/j.est.2020.101485>
 97. R. Kumar, R.K. Singh, A.R. Vaz, R. Savu, S.A. Moshkalev, Self-assembled and one-step synthesis of interconnected 3D network

- of Fe₃O₄/reduced graphene oxide nanosheets hybrid for high-performance supercapacitor electrode. *ACS Appl Mater Interfaces* **9**, 10 (2017). <https://doi.org/10.1021/acsami.6b14704>
98. R. Kumar, Rajesh Kumar Singh, Pawan Kumar Dubey, Dinesh Pratap Singh, Ram Manohar Yada, Self-assembled hierarchical formation of conjugated 3D cobalt oxide nanobead–CNT–graphene nanostructure using microwaves for high-performance supercapacitor electrode. *ACS Appl Mater Interfaces* **7**, 27 (2015). <https://doi.org/10.1021/acsami.5b04336>
 99. H.-J. RajeshKumar, SungjinPark, AnchalSrivastava, KwonOh, Graphene-wrapped and cobalt oxide-intercalated hybrid for extremely durable super-capacitor with ultrahigh energy and power densities. *Carbon* **79**, 192–202 (2014). <https://doi.org/10.1016/j.carbon.2014.07.059>
 100. R. Kumar, R.K. Singh, R. Savu, P.K. Dubey, P. Kumar, S.A. Moshkalev, Microwave-assisted synthesis of void-induced graphene-wrapped nickel oxide hybrids for supercapacitor applications. *RSC Advances* **6**(32), 26612–26620 (2016). <https://doi.org/10.1039/C6RA00426A>
 101. R. Kumar, S. Youssry, Kyaw Zay Ya, Wai Kian Tan, Go Kawamura, Atsunori Matsuda Kawamura, Atsunori Matsuda, Microwave-assisted synthesis of Mn₃O₄-Fe₂O₃/Fe₃O₄@rGO ternary hybrids and electrochemical performance for supercapacitor electrode. *J. Diamond and Related Materials* **101**, 107622 (2020). <https://doi.org/10.1016/j.diamond.2019.107622>
 102. R. Kumar, R. Matsuo, K. Kishida, M.M. Abdel-Galeila, Y. Suda, A. Matsuda, Homogeneous reduced graphene oxide supported NiO-MnO₂ ternary hybrids for electrode material with improved capacitive performance. *J Electrochimica Acta* **303**, 246–256 (2019). <https://doi.org/10.1016/j.electacta.2019.02.084>
 103. X. Wang, W.S. Liu, X. Lu, P.S. Lee, Dodecyl sulfate-induced fast faradic process in nickel cobalt oxide-reduced graphite oxide composite material and its application for asymmetric supercapacitor device. *J Mater Chem* **22**, 23114–23119 (2012). <https://doi.org/10.1039/c2jm35307e>
 104. Q. Li, C. Lu, C. Chen, L. Xie, Y. Liu, Y. Li, Q. Kong, H. Wang, Layered NiCo₂O₄/reduced graphene oxide composite as an advanced electrode for supercapacitor. *Energy Storage Mater* **8**, 59–67 (2017). <https://doi.org/10.1016/j.ensm.2017.04.002>
 105. Y.Z. Cai, W.Q. Cao, Y.L. Zhang, P. He, J.C. Shu, M.S. Cao, Tailoring rGO-NiFe₂O₄ hybrids to tune transport of electrons and ions for supercapacitor electrodes. *J. Alloys Compd.* **811**, 152011 (2019). <https://doi.org/10.1016/j.jallcom.2019.152011>
 106. A. Chebil, O. Kuzgun, C. Dridi, M. Ates, High power density supercapacitor devices based on nickel foam-coated rGO/MnCo₂O₄ nanocomposites. *Ionics (Kiel)* **26**, 5725–5735 (2020). <https://doi.org/10.1007/s11581-020-03713-3>
 107. A. Singh, S.K. Ojha, A.K. Ojha, Facile synthesis of porous nanostructures of NiCo₂O₄ grown on rGO sheet for high performance supercapacitors. *Synth. Met.* **259**, 116215 (2020). <https://doi.org/10.1016/j.synthmet.2019.116215>
 108. Y. Li, J. Jian, Y. Fan, H. Wang, L. Yu, G. Cheng, J. Zhou, M. Sun, Facile one-pot synthesis of a NiMoO₄/reduced graphene oxide composite as a pseudocapacitor with superior performance. *RSC Adv* **6**, 69627–69633 (2016). <https://doi.org/10.1039/c6ra13955h>
 109. Y. Luo, H. Zhang, D. Guo, J. Ma, Q. Li, L. Chen, T. Wang, Porous NiCo₂O₄-reduced graphene oxide (rGO) composite with superior capacitance retention for supercapacitors. *Electrochim Acta* **132**, 332–337 (2014). <https://doi.org/10.1016/j.electacta.2014.03.179>
 110. G. He, L. Wang, H. Chen, X. Sun, X. Wang, Preparation and performance of NiCo₂O₄ nanowires-loaded graphene as supercapacitor material. *Mater Lett* **98**, 164–167 (2013). <https://doi.org/10.1016/j.matlet.2013.02.035>
 111. L. Ma, X. Shen, H. Zhou, Z. Ji, K. Chen, G. Zhu, High performance supercapacitor electrode materials based on porous NiCo₂O₄ hexagonal nanoplates/reduced graphene oxide composites. *Chem Eng J* **262**, 980–988 (2015). <https://doi.org/10.1016/j.cej.2014.10.079>
 112. B. Rani, N.K. Sahu, Electrochemical properties of CoFe₂O₄ nanoparticles and its rGO composite for supercapacitor. *Diam. Relat. Mater.* **108**, 107978 (2020). <https://doi.org/10.1016/j.diamond.2020.107978>
 113. C.Y. Foo, H.N. Lim, M.A.B. Mahdi, K.F. Chong, N.M. Huang, High-performance supercapacitor based on three-dimensional hierarchical rGO/nickel cobaltite nanostructures as electrode materials. *J Phys Chem C* **120**, 21202–21210 (2016). <https://doi.org/10.1021/acs.jpcc.6b05930>
 114. Y. Xu, H. Xuan, J. Gao, T. Liang, X. Han, J. Yang, Y. Zhang, H. Li, P. Han, Y. Du, Hierarchical three-dimensional NiMoO₄-anchored rGO/Ni foam as advanced electrode material with improved supercapacitor performance. *J Mater Sci* **53**, 8483–8498 (2018). <https://doi.org/10.1007/s10853-018-2171-1>